AD_____

Award Number: W81XWH-11-1-0552

TITLE: *Inhibition of the Androgen Receptor Amino-Terminal Domain by a Small Molecule as Treatment for Castrate-Resistant Prostate Cancer*

PRINCIPAL INVESTIGATOR: Stephen R. Plymate

CONTRACTING ORGANIZATION: University of Washington, Seattle, WA 98195-9472

REPORT DATE: October 2013

TYPE OF REPORT: Annual

PREPARED FOR: U.S. Army Medical Research and Materiel Command
Fort Detrick, Maryland 21702-5012

REPORT DOCUMENTATION PAGE

Form Approved
OMB No. 0704-0188

1. REPORT DATE	2. REPORT TYPE	3. DATES COVERED
October 2013	Annual	15September2012–14September2013

4. TITLE AND SUBTITLE
"Inhibition of the Androgen Receptor Amino-Terminal Domain by a Small Molecule as Treatment for Castrate-Resistant Prostate Cancer"

5a. CONTRACT NUMBER

5b. GRANT NUMBER
W81XWH-11-1-0552

5c. PROGRAM ELEMENT NUMBER

6. AUTHOR(S)
Stephen R. Plymate

E-Mail: splymate@u.washington.edu

5d. PROJECT NUMBER

5e. TASK NUMBER

5f. WORK UNIT NUMBER

7. PERFORMING ORGANIZATION NAME(S) AND ADDRESS(ES)
University of Washington
Seattle, WA 98195-9472
(206) 543-4043 tel
(206) 685-1732 fax
osp@uw.edu

8. PERFORMING ORGANIZATION REPORT NUMBER

9. SPONSORING / MONITORING AGENCY NAME(S) AND ADDRESS(ES)
U.S. Army Medical Research and Materiel Command
Fort Detrick, Maryland 21702-5012

10. SPONSOR/MONITOR'S ACRONYM(S)

11. SPONSOR/MONITOR'S REPORT NUMBER(S)

12. DISTRIBUTION / AVAILABILITY STATEMENT
Approved for Public Release; Distribution Unlimited

13. SUPPLEMENTARY NOTES

14. ABSTRACT **-Purpose:** The hypothesis of this study is that EPI-001 that targets the AR NTD will inhibit AR-driven recurrence of prostate cancer resistant to current methods of androgen deprivation or blockade.
Scope: Aim 1 will determine the impact of EPI-001 on castration sensitive tumor regression and re-growth in LuCaP xenografts and on growth of their castration resistant forms. **Aim 2** will examine the impact of EPI-001 on castration sensitive and castration resistant growth of tumors with differing tumor androgen levels and differing ratios of ARv567es to full-length AR. **Aim 3** will elucidate the specific molecular mechanisms by which EPI-001 inhibits the activity of full-length AR and truncated ARv567es variants using in vitro models.
Progress: Tasks 1 and 3:We have completed the EPI-002 treatment in 5 xenograft lines in the second year of this study. These were done following castration and in castrate resistant growth states. Tasks 4 and 5: We have measured intratumoral androgen and found that they have a major impact on EPI—2 response.
IHC analysis of these tumors. A distinct AR variant transcriptome has been identified is suppressed by EPI-002.
Findings: We have clearly shown that EPI-001 and -002 can suppress the growth of AR-variant driven prostate cancers. We have also shown that Intratumoral androgens play a major role in determining response to N-terminal inhibition.
Significance: Based on these studies to this point as formulation of the compounds is optimized we would hope to move forward with application for FDA approval for Phase 1 clinical trials.

15. SUBJECT TERMS none provided

16. SECURITY CLASSIFICATION OF:			17. LIMITATION OF ABSTRACT	18. NUMBER OF PAGES	19a. NAME OF RESPONSIBLE PERSON
a. REPORT	b. ABSTRACT	c. THIS PAGE			USAMRMC
U	U	U	UU	31	19b. TELEPHONE NUMBER *(include area code)*

Table of Contents

Page

Introduction……..……..…..4

Body……..4-6

Key Research Accomplishments…….. 7

Reportable Outcomes…… 7

Conclusion…… 7

References…….7

Appendices…… N/A

Introduction: During this past year the role of AR splice variants in association with resistance to abiraterone and enzalutamide has become increasingly clinically relevant. Several studies including those of a collaborator on our DOD –transformative proposal, Dr. Jun Luo at Johns Hopkins University have provided important clinical correlative data showing that the appearance of androgen receptor splice variants in association with the resistance that is increasingly developing in our patients to these new C-terminal AR agents. In addition as we will point out in this report, we now show that generation of AR-splice variants occurs at the level of preMRNA splicing and does not require the presence of intragenic rearrangements of the AR gene. We have shown that EPI compounds markedly inhibit tumor growth in which the tumors are devoid of androgens and are driven by AR splice variants. Importantly, the clinical appearance of these tumors may indicate that a paradigm shift in our approach to castration resistant disease may be needed. Finally, in this proposal we originally began using EPI-001. This compound is a mixture of four stereoisomers. We determined that the activity of the compound was associated with the specific isomer, EPI-002 (1). Thus we are now using this compound in the studies and herein is referred to as EPI-002.

Body:

Aim 1 will determine the impact of EPI-001 on castration sensitive tumor regression and re-growth in LuCap xenografts and on growth of their castration resistant forms.

LuCaP 86.2 xenograft and epi – The data on this xenograft was presented in the previous report and as shown this human prostate cancer xenograft was resistant to enzalutamide but was very sensitive to EPI-001.Sunsequent analysis of RNA from these xenografts showed a decrease in AR^{v567es} distinct targets UBE2C and UGT2B17 when treated with EPI-001. Importantly it has been shown that LuCaP 86.2 from which AR^{v567es} has an intragenic rearrangement of the AR gene and is programmed to produce AR^{v567es} and does not generate AR-V7.This is an important finding because we have shown that AR^{v567es} is transported

LuCaP 136 and epi – The data on LuCaP136 were also presented in the last report. Importantly we saw that this xenograft was also growth suppressed by enzalutamide. When we first reported this xenograft in 2010 it had higher intratumoral levels of DHT than T and our collaborator, Scott Dehm, had found an intragenic rearrangement similar to that in LuCaP 86.2. However; when we examined the LuCaP 136 tumors that were suppressed by enzalutamide and EPI-001, we say only AR-V7 but predominantly AR-FL and on castration higher levels of testosterone than dihydrotestosterone as the intratumoral androgen. Furthermore, the intragenic rearrangement of AR had been lost. Thus this is an important finding because it shows that in EPI-001 can suppress tumor growth in which the dominant receptor is AR-FL. The importance of the switch in intratumoral steroid from DHT to T is of interest but the importance in the response to various agents has yet to be determined.

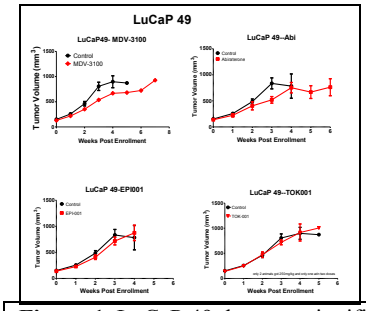

Figure 1. LuCaP 49 does not significantly decrease growth in response N- or C-terminal AR inhibitors.

LuCaP 49 and EPI - LuCaP 49 is a neuroendocrine tumor that does not contain AR and is thus unresponsive to either N-terminal inhibition by EPI-001 or LBD inhibition by enzalutamide (MDV-3100), abiraterone or Tok-001. Although a negative finding this is an important finding since it shows no off target effects on tumor suppression by EPI compounds.

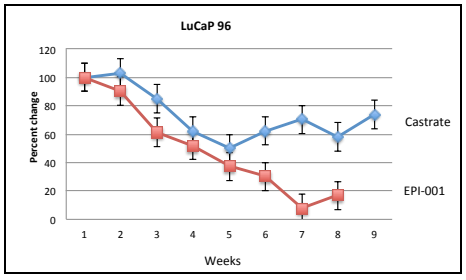

Figure 2. LuCaP 96 shows some response to castration alone but a better response to EPI-001. Although originally thought to be driven primarily by AR-FL recent RNA-seq analysis demonstrated that over 30% of the LuCaP 96 AR is a constitutively active AR-variant.

LuCaP 96 and EPI – In figure 2 we see the results of treatment of the LuCaP 96 xenograft. Although there is an initial response to castration, the response is muted over time

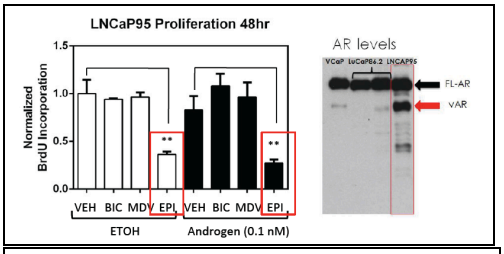

Fig. 3. LNCaP95 cells express both AR–FL, AR-V7 and AR^{v567es} as seen in the Western blot (right). They grow in the absence of androgen, are not suppressed by inhibiting the LBD with bicalutamide or MDV but proliferation is inhibited by the N-terminal inhibitor EPI-002.

and the response is significantly greater to EPI. We have subsequently performed RNA-seq on this xenograft and found that it contains >30% AR-splice variants that are forms of AR^{v567es} such that not are detected by qtrtPCR primers used for AR^{v567es} but may account for a significant amount of resistance to castration. Of further interest, testosterone as opposed to DHT , is the primary intratumoral androgen in LuCaP96 post castration and as we have seen in LuCaP 136 may provide additional information as to the response to EPI compounds.

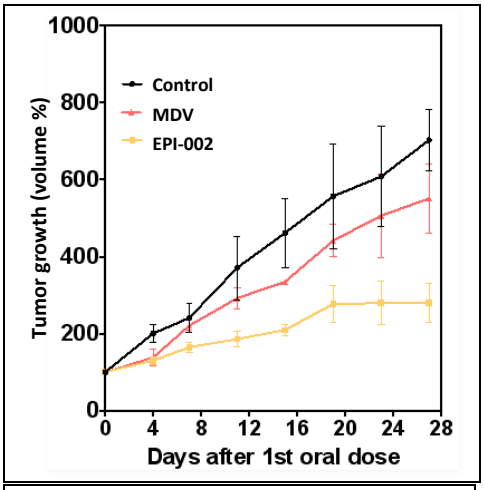

Figure 4. LNCaP 95 cells grown in castrateSCID mice treated with vehicle, enzalutamide (MDV) (30uM), or EPI-002 (50 mgm/kg) per gavage daily.

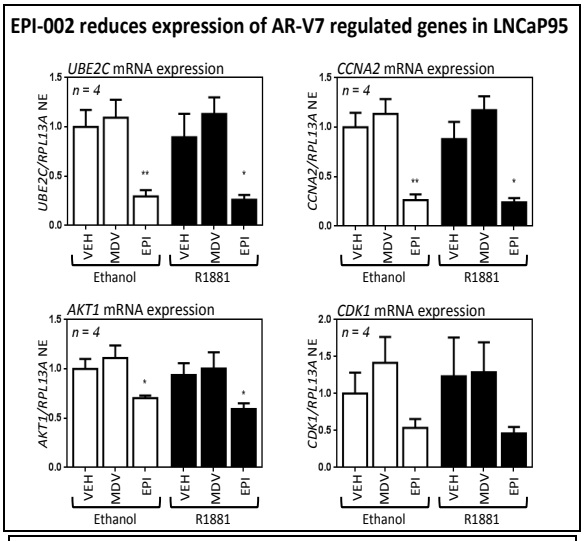

Figure 5. AR-variant distinct genes in variant drivenLNCaP 95 cells are suppressed by EPI-002 but not enzalutamide (MDV).

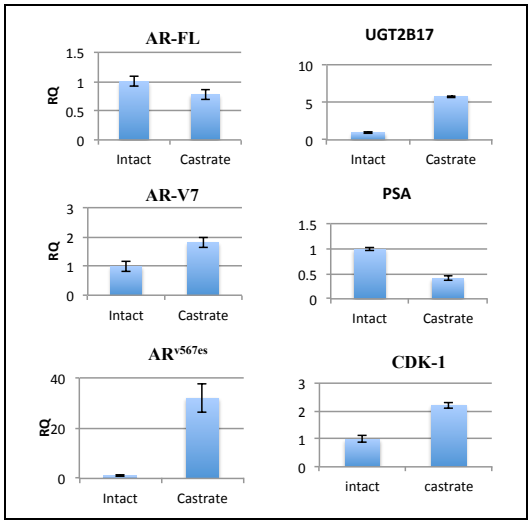

Figure 6. RtPCR of AR-FL, AR-V7, AR^{v567es}, and downstream AR genes in LnCaP 95 xenografts in intact or castrate mice.

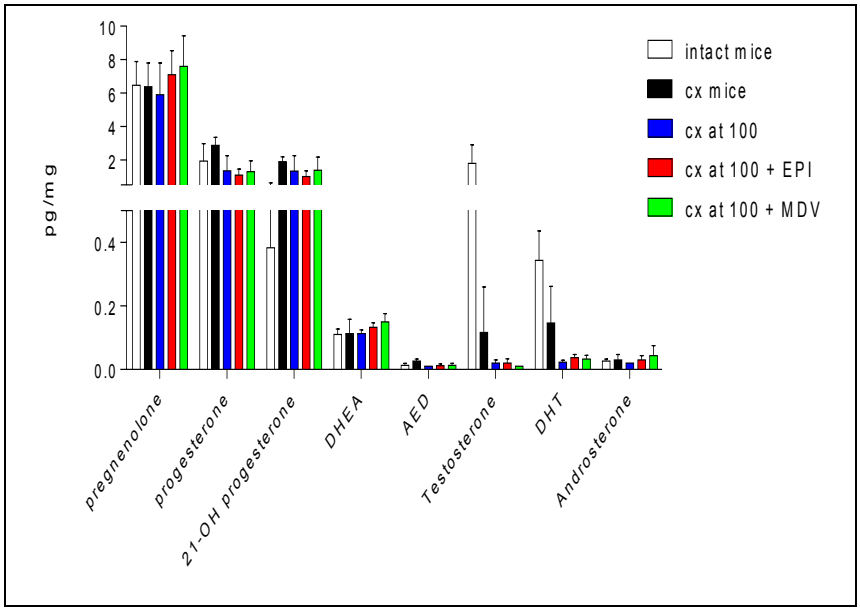

Aim 2 will examine the impact of EPI-001 on castration sensitive and castration resistant growth of tumors with differing tumor androgen levels and differing ratios of ARv567es to full-length.

Figure 7. Intratumoral steroid levels LNCaP 95xenografts treated as indicated. Tumors from Intact mice were removed at 10 weeks after implantation, cx mice at 7 weeks, and cx 100 at 4 weeks after start of treatment. Note that long-term castrate mice had some intratumoral androgen present, presumably due to intracrine androgen synthesis.

LnCaP 95 and EPI – In figure 3 we show that LNCaP 95 cell express high endogenous levels of AR-V7 as well as the AR-V7 transcriptome. Furthermore we have also shown, that as opposed to LNCaP parental cells that when grown as xenografts have suppressed growth following castration, the LNCaP 95 cells grow best when placed in castrate mice and their growth is suppressed when placed in intact mice or when androgens are replaced if they are grown in castrate mice. Thus they are androgen suppressed. Additionally, they are resistant to bicalutamide and enzalutamide, figure 3. However, when grown in castrate mice LNCaP 95 growth suppressed by the addition of EPI-002, figure 4, and the AR-variant transcriptome genes are suppressed, figure 5. In contrast, when LNCaP 95 cells are grown in the castrate host there is a marked increase in AR^{v567es} and

variant distinct genes. Whereas EPI-002 blocks the rise in variant genes inspite of the marked increase in AR^{v567es}, figure 6.

Steroid data. We have already commented on the steroid measurements in the xenografts. In addition, in figure **7** we show the intratumoral steroid levels from the LNCaP 95 xenografts. In the intact mice, in spite of the elevated levels of steroid glucuronidating genes, there is still a significant level of T and DHT that decreases following castration. However, those tumors that do occur at a later time point (cx mice) do appear to generate intra-tumoral steroids as opposed to those castrated at the earlier time point (cx at 100). Importantly, the regrowth after initial castration is not dependent on ligand but is dependent on the AR-variant as shown by growth suppression with EPI-002.

Aim 3 will elucidate the specific molecular mechanisms by which EPI-001 inhibits the activity of full-length AR and truncated ARv567es variants using in vitro models.

Splicing data For V7 and $AR^{v567es-}$ during the past funding period we have also examined how AR variants are made when there are no intragenic rearrangements of the AR-gene. We have published the splicing mechanisms for AR-V7 (2). In figures 8 and 9 we see our unpublished data on the mechanism for generation of the exon skipping variant AR^{v567es} from preMRNA. In this case the splicing inhibitor, polypyrimidine tract-binding protein (PTB), blocks splicing between exons 4 and 5 of the AR. The next strongest splice site is to exon 8. However, because there is a frame-shift, exon 8 has a stop codon after ten amino acids. In addition to the generation of AR^{v567es} PTB inhibits formation of the full-length AR, figure 8. The schema demonstrating PTB activity in the regulation of RNA-splicing is noted in Figure 10.

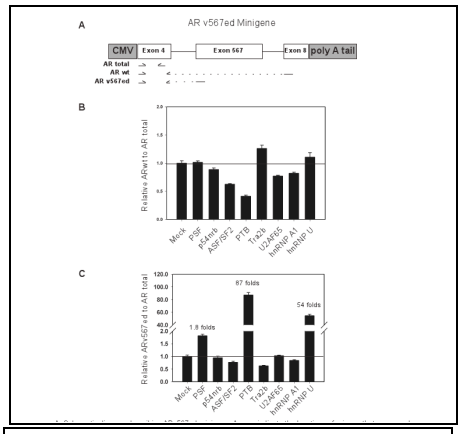

Figure 8. Plasmids expressing the splicing factors noted were added to M12 cells transfected with the AR^{v567es} minigene. As shown PTB increased AR^{v567es} and decreased AR-FL.

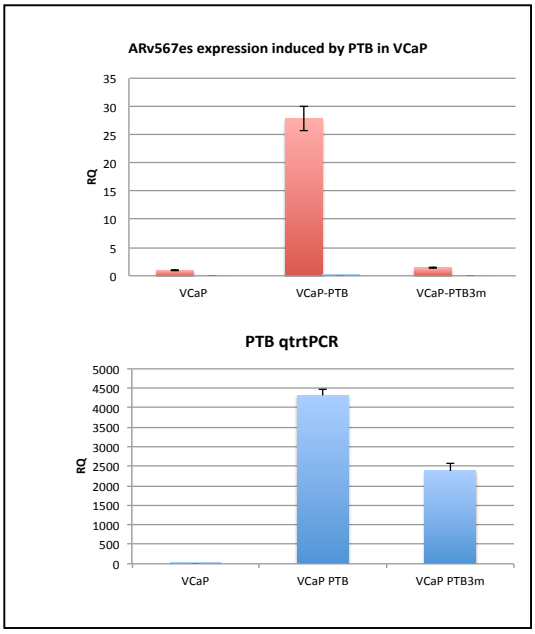

Figure 9. PTB expressed in VCaP cells induces splicing of endogenous AR preMRNA to make AR^{v567es}. Mutated PTB (PTB3m) has no effect.

Potential problems – One problem that has occurred during the last funding period has been some variation in solubility of EPI-002 between batches. This has slowed the xenograft work; however, we have now solved this problem and-expect the next year's mouse work to proceed at a more rapid pace.

Progress towards clinic – Finally, although clinical trial support has is not part of this synergy proposal, the work accomplished in this proposal has led to discussions and design to move an EPI compound forward into phase1 clinical trial. We hope to be at this point by the end of this next funding period with work based on this proposal.

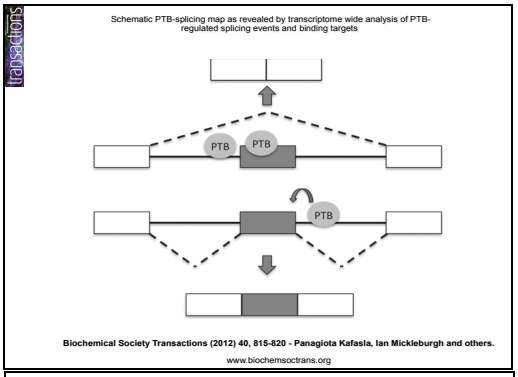

Figure 10. Schema of PTB splicing activity that leads to exon skipping variant.

Key Research Accomplishments

- **EPI-001 and 002 inhibits human xenograft tumor growth in the absence of androgen and the presence of AR-constitutively active splice variants.**
- **EPI compounds have no efficacy against neuroendocrine human LuCap xenografts that do not express the androgen receptor**
- **EPI- compounds are effective in human prostate cancer xenografts in which androgens are depleted and are now driven by AR splice variants.**
- **Generation of AR constitutively active variants occurs at the level of AR-preMRNA without genomic rearrangement of the AR gene.**

Reportable outcomes:

1. Myung JK, Banuelos CA, Garcia Fernadez J, Mawji N, Wang J, Tien AH, Tavakoli I, Yang YC, Haile S, McEwan I, Plymate S, Andersen RJ, Sadar MD 2013 EPI small molecules covalently bind intrinsically disordered N-terminal domain of the androgen receptor to inhibit the growth of castration-resistant prostate cancer. J Clin Invest. 2013 Jun 3. doi:pii: 66398. 10.1172/JCI66398. [Epub ahead of print] PMID:23722902
2. Liu LL, Xie N, Sun S, Plymate S, Mostaghel E, Dong X. Mechanisms of androgen receptor splicing in prostate cancer cells. Oncogene. 2013 Jul 15. doi: 10.1038/onc.2013.284. [Epub ahead of print] PMID:23851510

Funding applied for based on this award:
NIH- SPORE- Program – PNWSPORE
SPORE PI- P. Nelson,Plymate PI Project 5 (2 months)
Androgen Receptor in Prostate Cancer Progression
2013-2018
$168,000 current yr-
$840,000 total

Conclusion: The results of this past year's funding confirms the ability of EPI compounds to be relevant compounds to develop for the clinic as agents to treat castrate-resistant (lethal) forms of prostate cancer, especially when associated with AR- splice variants. Thus the results of these studies lead to our further development of the EPI-compounds as important medical products for the treatment of advanced prostate cancer. Scientifically, these studies demonstrate that the N-terminus of the androgen receptor is an important driver of prostate cancer in the absence of ligand.

References:

1. Myung JK, Banuelos CA, Garcia Fernadez J, Mawji N, Wang J, Tien AH, Tavakoli I, Yang YC, Haile S, McEwan I, Plymate S, Andersen RJ, Sadar MD 2013 EPI small molecules covalently bind intrinsically disordered N-terminal domain of the androgen receptor to inhibit the growth of castration-resistant prostate cancer. J Clin Invest. 2013 Jun 3. doi:pii: 66398. 10.1172/JCI66398. [Epub ahead of print] PMID:23722902
2. Liu LL, Xie N, Sun S, Plymate S, Mostaghel E, Dong X. Mechanisms of androgen receptor splicing in prostate cancer cells. Oncogene. 2013 Jul 15. doi: 10.1038/onc.2013.284. [Epub ahead of print] PMID:23851510

Appendices: 2 papers

Supporting Data: All supporting figures have been included in the text with appropriate figure numbers and labels.

Research article

An androgen receptor N-terminal domain antagonist for treating prostate cancer

Jae-Kyung Myung,[1] Carmen A. Banuelos,[1] Javier Garcia Fernandez,[2] Nasrin R. Mawji,[1] Jun Wang,[1] Amy H. Tien,[1] Yu Chi Yang,[1] Iran Tavakoli,[1] Simon Haile,[1] Kate Watt,[3] Iain J. McEwan,[3] Stephen Plymate,[4] Raymond J. Andersen,[2] and Marianne D. Sadar[1]

[1]Genome Sciences Centre, British Columbia Cancer Agency, Vancouver, British Columbia, Canada. [2]Chemistry and Earth, Ocean, and Atmospheric Sciences, University of British Columbia, Vancouver, British Columbia, Canada. [3]School of Medical Sciences, University of Aberdeen, Aberdeen, United Kingdom. [4]Department of Medicine, University of Washington, Harborview Medical Center, Seattle, Washington, USA.

Hormone therapies for advanced prostate cancer target the androgen receptor (AR) ligand-binding domain (LBD), but these ultimately fail and the disease progresses to lethal castration-resistant prostate cancer (CRPC). The mechanisms that drive CRPC are incompletely understood, but may involve constitutively active AR splice variants that lack the LBD. The AR N-terminal domain (NTD) is essential for AR activity, but targeting this domain with small-molecule inhibitors is complicated by its intrinsic disorder. Here we investigated EPI-001, a small-molecule antagonist of AR NTD that inhibits protein-protein interactions necessary for AR transcriptional activity. We found that EPI analogs covalently bound the NTD to block transcriptional activity of AR and its splice variants and reduced the growth of CRPC xenografts. These findings suggest that the development of small-molecule inhibitors that bind covalently to intrinsically disordered proteins is a promising strategy for development of specific and effective anticancer agents.

Introduction

Intrinsically disordered proteins (IDPs) are prevalent in eukaryotes and are associated with cancer, diabetes, and neurodegenerative and cardiovascular disorders. The lack of structure may be throughout the entire protein, or the protein may contain substantial regions of disorder. These proteins are involved in signaling and gene regulation, with protein-protein interactions being central to their mechanism. IDPs have flexibility, thereby providing the plasticity to enable interactions with multiple partners where high-specificity and low-affinity interactions are critical for reversible binding (1). IDPs such as c-myc, p53, EWS-Fli1, and androgen receptor (AR) N-terminal domain (NTD) play central roles in cancer, thereby making them ideal targets of anticancer therapies. To our knowledge, no drug targeting an IDP has reached clinical testing, nor has the binding of any small-molecule inhibitor to an NTD of a steroid receptor ever been described.

Prostate cancer recurs in 20%–40% of patients with high-grade disease after primary treatment. For these patients, androgen ablation therapy is employed, using approaches that target the AR ligand-binding domain (LBD), including antiandrogens that all directly bind LBD, or that reduce levels of circulating and tissue androgens with LHRH/GnRH analogs and CYP17 inhibitors (2). Although these therapies are initially effective in 90% of patients, the disease will inevitably recur as lethal castration-resistant prostate cancer (CRPC). In spite of castrate levels of androgen, development of CRPC is considered to be causally related to continued transactivation of AR by mechanisms that may include amplification or overexpression of AR (3, 4), gain-of-function mutations that allow AR to be activated by steroids or antiandrogens (5, 6), ligand-independent activation of the AR NTD by interleukin-6 or kinases (7–10), overexpression of AR coactivators (11–14), intracrine signaling by increased intratumoral androgens (15), and expression of constitutively active splice variants of AR that lack the C-terminal LBD and are correlated with poor prognosis (16–19). Patients succumb to metastatic CRPC usually within 2 years of onset. In vivo proof-of-principle demonstration of therapeutic response by targeting the AR NTD in CRPC was first shown with decoy proteins (20), and then with EPI-001, a small molecule that inhibits transactivation of AR NTD (21).

AR is a member of the steroid receptor family of transcription factors that share structurally conserved domains consisting of a DNA-binding domain (DBD), LBD, NTD, and a hinge region that contains a nuclear localization sequence. Unlike the intrinsically disordered NTD, the DBD and LBD of AR are intrinsically ordered with resolved crystal structures. Consistent with the properties of IDPs, AR interacts with more than 160 proteins (22), and protein-protein interactions with the activation function-1 (AF1) region in the NTD are essential for AR transcriptional activity (23–26). AR NTD has less than 15% homology with other steroid receptors that also have predominantly intrinsically disordered NTDs (27–31). Malleability of intrinsically disordered NTDs of these transcription factors is crucial for their function that requires interactions with many binding partners. Since AR NTD lacks enzymatic activity or rigid binding clefts for receptor-ligand interaction, small-molecule inhibitors would work by disruption of essential protein-protein interactions from active transcriptional complexes. The AR transcriptional complex is composed of many proteins, including CBP and RAP74 (26, 32). Our previous investigation showed that EPI-001 inhibits these protein-protein interactions by attenuation of AR transcriptional activity, increased apoptosis, and decreased proliferation, all of which are essential for CRPC tumor maintenance (21). Small-molecule inhibitors of the AR

Conflict of interest: Carmen A. Banuelos, Javier Garcia Fernandez, Nasrin R. Mawji, Jun Wang, Raymond J. Andersen, and Marianne D. Sadar are coinventors of EPI; however, Raymond J. Andersen and Marianne D. Sadar had to waive all rights to inventor royalties. Stephen Plymate, Raymond J. Andersen, and Marianne D. Sadar are consultants to ESSA Pharma Inc. Carmen A. Banuelos, Javier Garcia Fernandez, Nasrin R. Mawji, Jun Wang, Stephen Plymate, Raymond J. Andersen, and Marianne D. Sadar own ESSA Pharma Inc. stock.

Citation for this article: *J Clin Invest.* 2013;123(7):2948–2960. doi:10.1172/JCI66398.

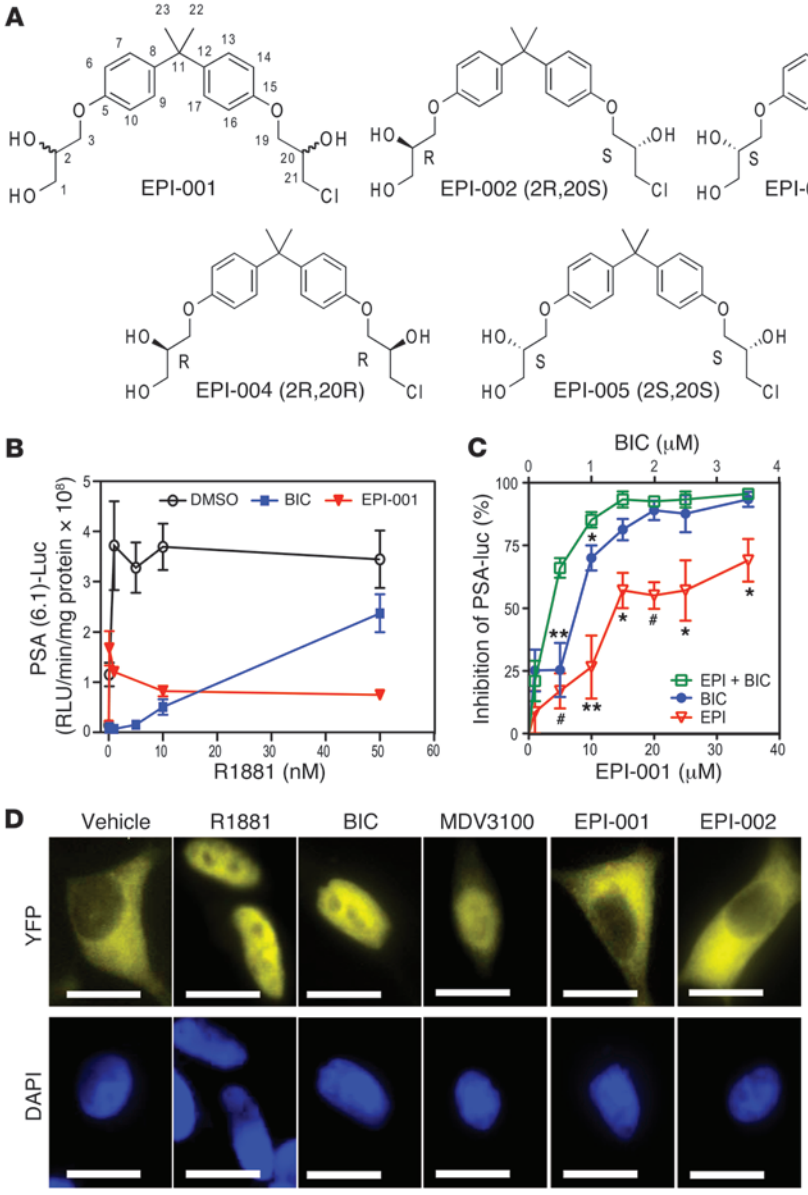

Figure 1
Unique mechanism of action of EPI compared with antiandrogens. (**A**) Structures of EPI-001 mixture and stereoisomers. (**B**) AR transcriptional activity, measured in LNCaP cells transiently transfected with the PSA(6.1kb)-luciferase reporter and treated with vehicle (DMSO), 10 μM bicalutamide (BIC), or 25 μM EPI-001 for 1 hour followed by increasing concentrations of R1881 for 48 hours. (**C**) Effect of bicalutamide (0.1–3.5 μM) and EPI-001 (1–35 μM), alone or in combination (1:10 ratio), on androgen-induced AR transactivation in LNCaP cells transfected with the PSA(6.1kb)-luciferase reporter. (**D**) Nuclear translocation of AR in LNCaP cells transfected with AR-YFP in serum-free conditions for 24 hours prior to treatment with 1 nM R1881, 10 μM bicalutamide, 10 μM MDV3100, 25 μM EPI-001, or 25 μM EPI-002 for 4 hours. DAPI staining shows the location of the nucleus. Scale bars: 10 μm. Data are mean ± SEM. $^{*}P < 0.05$; $^{**}P < 0.01$; $^{\#}P < 0.001$.

NTD may overcome the shortcomings of current therapies targeting the AR LBD for CRPC and represent the first in a new class of antitumor therapies against IDPs being clinically developed.

Targeting IDPs by small molecules to block protein-protein interactions is a rapidly evolving field, as the importance of these proteins in disease becomes established. The plasticity of IDPs with labile regions that can be shaped by their environment and interactions provides potential for small-molecule binding (33). However, the general property of reversible, low-affinity binding of IDPs to many interacting partners to facilitate the exchange of binding partners may forecast a requirement of irreversible binding for any small-molecule inhibitor to have a sustained therapeutic effect. On the basis of these observations, the mechanism of targeting the AR NTD by EPI-001 and its analogs may provide precedent in drug development against other IDPs. Here, we showed that EPI (a) bound covalently to AF1 in the intrinsically disordered AR NTD and did not bind to denatured AF1; (b) had no stereospecificity for covalent binding to AR in living cells; (c) inhibited constitutively active AR splice variants lacking LBD that are suspected in resistant mechanisms to current therapies; (d) was unique from antiandrogens, in that EPI did not cause AR nuclear translocation and its efficacy was not compromised by elevated levels of androgen; and (e) had excellent pharmacokinetic properties. These findings suggest that EPI compounds are promising small molecules to develop therapeutics for CRPC.

Results

EPI has a unique mechanism of action. EPI-001 is an effective and specific inhibitor of AR transcriptional activity (21). EPI-001 has 2 chiral centers and is a mixture of 4 stereoisomers, EPI-002 (2R, 20S), EPI-003 (2S, 20R), EPI-004 (2R, 20R), and EPI-005 (2S, 20S) (Figure 1A). Consistent with EPI compounds targeting the NTD, inhibition of AR activity could not be competed away with increasing concentrations of androgen, as shown with endoge-

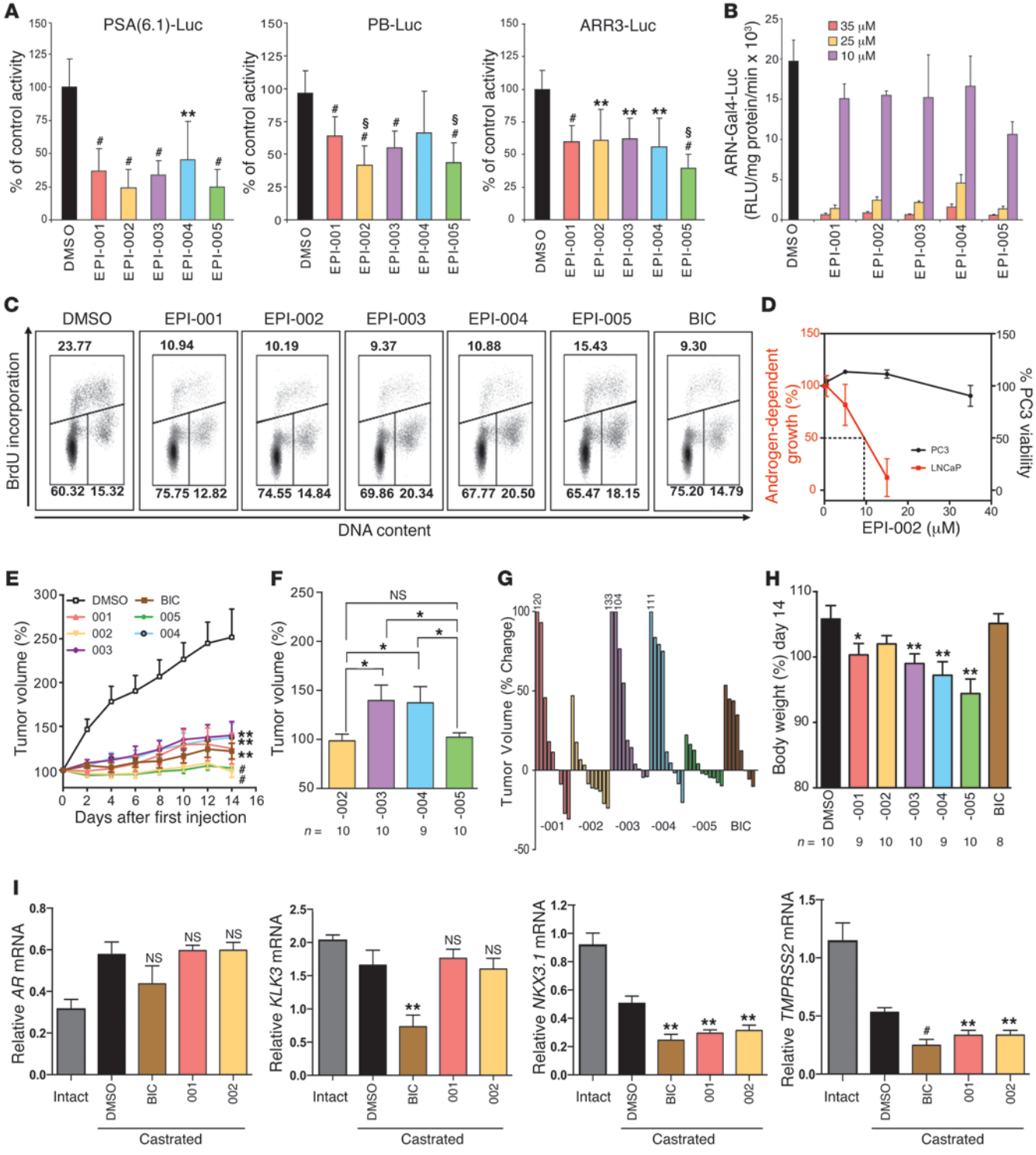

Figure 2
Stereospecificity of EPI-001 on AR transcriptional activity. (**A**) LNCaP cells were transfected with luciferase reporters and treated with 1 nM R1881 for 48 hours. Data represent percent of control (DMSO). $^{**}P < 0.01$, $^{\#}P < 0.001$ vs. DMSO; $^{\S}P < 0.05$ vs. EPI-001. (**B**) AR NTD transactivation assay in LNCaP cells treated with indicated concentrations of EPI-001 stereoisomers prior to treatment with 50 μM forskolin or DMSO. (**C**) Inhibition of androgen-induced DNA synthesis in LNCaP cells by stereoisomers of EPI-001 (25 μM) or bicalutamide (10 μM) treated with 0.1 nM R1881 for 48 hours. Data represent percent S-phase cells staining positive for BrdU incorporation (bivariate flow cytometric) from a representative experiment. (**D**) Effects of EPI-002 on androgen-dependent proliferation of LNCaP cells treated with R1881 compared with PC3 cell viability. (**E**) Decrease of CRPC LNCaP tumor volume in castrated mice administered EPI-001 mixture and stereoisomers (i.v. 50 mg/kg body weight) every other day for a total of 7 doses. Bicalutamide (10 mg/kg body weight) was administered daily by oral gavage. (**F**) Comparison of tumor volume from treatment with single stereoisomers. (**G**) Percent change of tumor volume of individual animals treated with stereoisomers or bicalutamide. (**H**) Body weight change at day 14 versus day 0. (**I**) mRNA levels of full-length *AR* and androgen-regulated genes measured from the LNCaP xenografts. Intact, noncastrated control group ($n = 3$). Values were normalized to housekeeping gene *RPL13A*. Data are mean ± SD (**A** and **B**) or mean ± SEM (**D**–**F**, **H**, and **I**). $^{*}P < 0.05$; $^{**}P < 0.01$; $^{\#}P < 0.001$.

nous AR in LNCaP human prostate cancer cells transfected with the AR-driven PSA(6.1kb)-luciferase reporter, which is induced by the synthetic androgen R1881 (Figure 1B). Antiandrogens, such as bicalutamide and MDV3100, bound to the AR LBD to act as competitive inhibitors of androgen. As expected, when the concentrations of R1881 were increased, the ability of bicalutamide to inhibit AR activity was significantly reduced. At R1881 concentrations of 1–5 nM, bicalutamide (10 μM) completely blocked AR activity, measured as PSA-luciferase activity. However, at 50 nM R1881, this same concentration of bicalutamide was a poor inhibitor, at only approximately 30% inhibition. EPI-001 (25 μM) inhibited AR activity consistently, regardless of increasing levels of androgen, and at 50 nM R1881, EPI-001 still inhibited AR activity by approximately 80%. Elevated androgen level also reverses the inhibitory effects of MDV3100 on androgen-dependent proliferation of VCaP cells (34). This general property of antiandrogens competing with androgen for the LBD may forecast their potential failure when androgen becomes elevated in CRPC and also with resistance to abiraterone (15, 35). These data support that EPI does not bind to the AR LBD, consistent with data from the fluorescent polarization assay showing no competition with the fluoromone for the AR LBD (Supplemental Figure 1A; supplemental material available online with this article; doi:10.1172/JCI66398DS1), as previously reported (21). Moreover, no binding to LBD was detected with related steroid hormone receptors, as expected, based on previous studies confirming specificity of EPI-002 for blocking transcriptional activity of AR at concentrations that had no effect on the transcriptional activities of related steroid hormone receptors (21).

Androgen and antiandrogens bind the structured LBD that is accessible for binding ligands due to interaction with chaperones. The AR NTD, an IDP, interacts with many proteins, which suggests that the binding site of EPI may not be continuously accessible throughout the cell cycle. Since the AR LBD and the AR NTD represent completely different drug targets, one being a structured binding pocket and the other being an IDP, this would suggest that drug combinations may yield additive or synergistic responses. Consistent with this theory, a drug combination study using a fixed ratio (1:10) of EPI-001 (1–35 μM) with a suboptimal concentration of bicalutamide (0.1–3.5 μM) significantly improved inhibition of androgen-induced AR activity compared with inhibition by the individual inhibitors (Figure 1C). A suboptimal concentration of bicalutamide (0.5 μM) inhibited androgen-induced AR activity by approximately 27%, similar to the 22% inhibition achieved with 5 μM EPI-001. A cocktail of 0.5 μM bicalutamide and 5 μM EPI-001 significantly reduced AR activity by 70%, thereby supporting combination therapy as a potential strategy for targeting both LBD and NTD.

Another mechanism potentially underlying clinical failure of antiandrogens may involve nuclear translocation of AR. In the absence of androgen, AR is predominantly cytosolic. Antiandrogens, including MDV3100 and ARN-509, induce nuclear translocation of AR (34, 36, 37). As expected, R1881, bicalutamide, and MDV3100 all induced AR nuclear translocation, whereas EPI-001 and EPI-002 did not, with AR remaining in the cytosol (Figure 1D). These data support that EPI-001 has a different mechanism of action compared with antiandrogens and highlight aspects of antiandrogens that may contribute to their clinical failure.

Optimal chirality of EPI for inhibition of AR transcriptional activity. Drug enantiomers and/or stereoisomers are considered different chemical compounds that may vary considerably in potency, pharmacological activities, off-targets, and pharmacokinetics. In fact, with a mixture of 4 stereoisomers, as much as 75% of the mixture could be considered contaminants, with potentially only 1 stereoisomer possessing the desirable qualities necessary for efficacy. Due to the potential differences in biological activity among stereoisomers, the FDA requires that each stereoisomer be evaluated when developing chiral drugs. Therefore, dose response curves using PSA-luciferase reporter were used to calculate IC_{50} values for EPI-001 and each stereoisomer (Supplemental Figure 1B). EPI-001 had an IC_{50} of 12.63 ± 4.33 μM, whereas the value for EPI-002 was 7.40 ± 1.46 μM (Supplemental Table 1). Significant differences between stereoisomers were only observed between EPI-002 and EPI-003 and between EPI-002 and EPI-004. Reporter specificity was investigated using 3 well-characterized AR-driven reporter gene constructs that included PSA-, probasin- (PB-), and ARR3-luciferase reporters. All stereoisomers inhibited the transcriptional activity of AR, as measured using these reporters (Figure 2A). Significant differences compared with EPI-001 were shown for EPI-002 with PB-luciferase, EPI-005 with PB-luciferase, and EPI-005 with ARR3-luciferase. EPI-002 and EPI-005 decreased AR activity to approximately 24% for PSA(6.1kb)-luciferase and 40% for PB-luciferase; for ARR3-luciferase, EPI-002 inhibited AR activity to 61%, whereas EPI-005 inhibited AR activity to 38% (Supplemental Table 1). All stereoisomers inhibited transactivation of the AR NTD induced by forskolin (Figure 2B).

EPI analogs decrease proliferation and S-phase. Cell cycle analysis was performed on androgen-dependent growth of LNCaP cells in response to EPI. In the absence of EPI analogs (i.e., DMSO vehicle), approximately 21% of cells were in S-phase in response to androgen (Supplemental Table 2). BrdU uptake in S-phase cells was decreased about 2-fold or more after exposure to each stereoisomer, with a concomitant increase of cells in G1-phase (Figure 2C and Supplemental Table 2). There were no statistical differences among the individual stereoisomers, with each inhibiting androgen-depen-

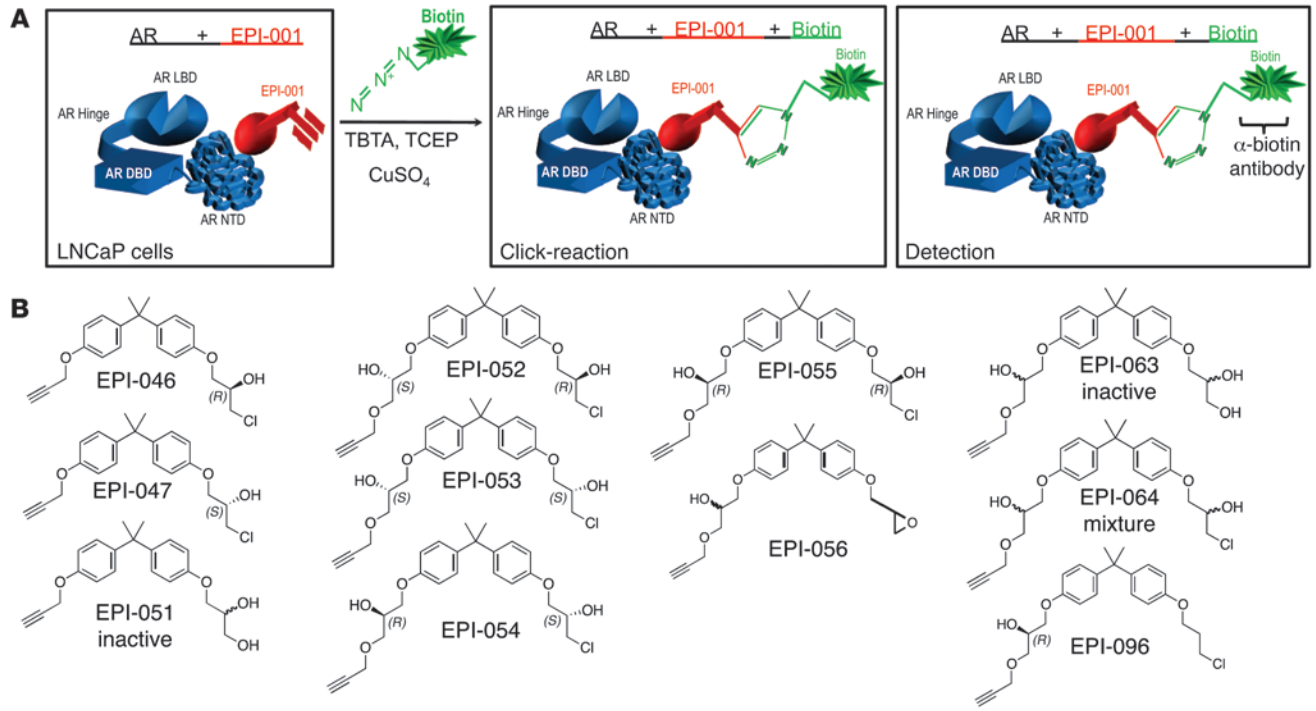

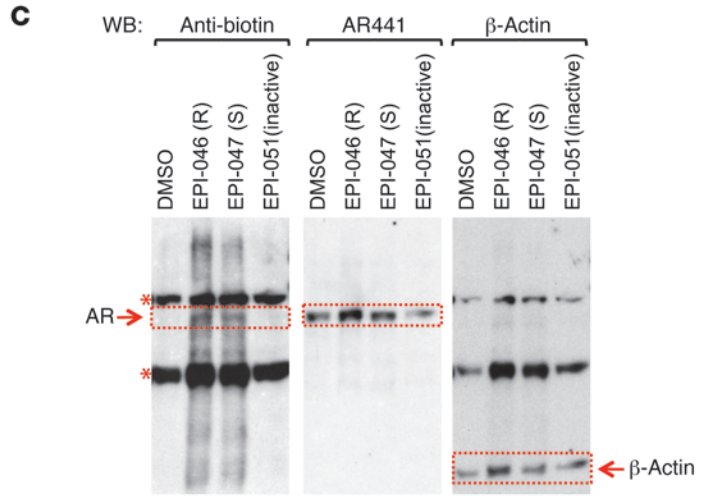

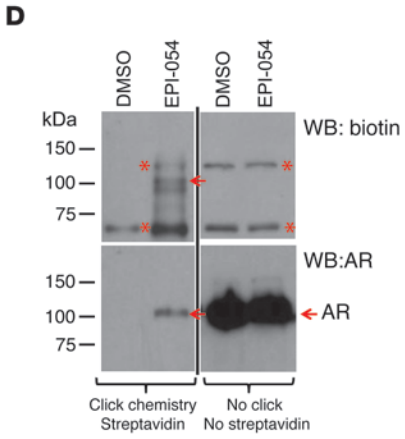

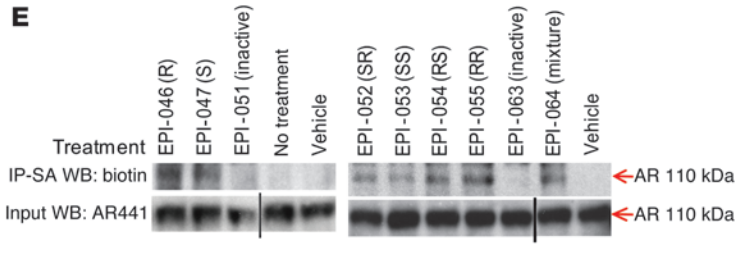

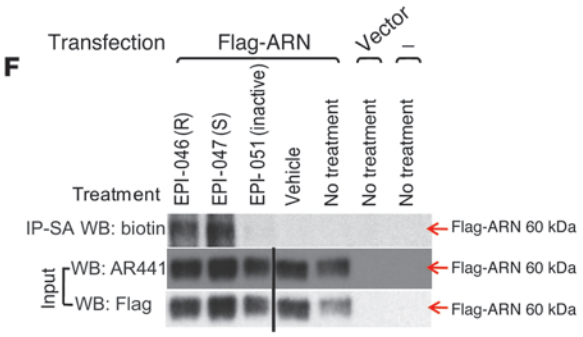

Figure 3
Covalent binding of EPI-001 probes to AR in cells. (**A**) Click-chemistry experiment. (**B**) EPI probes used for Click-chemistry. (**C**) LNCaP cells treated with EPI-046, EPI-047, and EPI-051 were lysed prior to Click-chemistry. Biotin-labeled probes covalently bound to cellular proteins were detected using an antibody against biotin (left), and AR protein was detected using an antibody against AR (middle). β-actin is a loading control (right). Dotted red outlines denote AR and β-actin bands, as indicated. (**D**) Western blot analysis of biotin-labeled probes covalently bound to cellular proteins from LNCaP cells treated with EPI-054 before (right) or after Click-chemistry and streptavidin enrichment (left). Gels were probed using anti-biotin or anti-AR antibodies, as indicated. Arrows denote bands corresponding to AR (110 kDa). (**E**) LNCaP cells treated with EPI chiral probes were lysed prior to Click-chemistry, enriched using streptavidin, and probed using anti-biotin antibody (top). AR levels prior to Click-chemistry were detected using anti-AR441 antibody (input; bottom). (**F**) Cells transfected with FLAG-AR NTD or vector were treated with EPI analogs. Proteins were detected using anti-biotin, anti-AR NTD, or anti-FLAG antibodies following Click-chemistry and streptavidin enrichment (top) or cell lysates before Click-chemistry (input; middle and bottom). Asterisks denote proteins that were also detected with anti-biotin antibody in DMSO samples not treated with EPI-probes. Lanes in **D**–**F** were run on same gel but were noncontiguous (black lines).

dent DNA synthesis associated with proliferation. The specificity of EPI-001 for blocking AR-dependent growth, while having no effect on the proliferation of cells that do not depend on AR for growth and survival, was previously reported (21). Here, EPI-002 also had no effect on the viability of PC3 human prostate cancer cells that do not express functional AR, at concentrations that reduced AR-dependent proliferation of LNCaP cells (Figure 2D).

Stereoisomers of EPI-001 inhibit CRPC. In vitro, EPI-002 and EPI-005 were the most potent stereoisomers in their ability to block AR transcriptional activity depending upon the reporter. To determine whether these in vitro responses could predict superior antitumor activity in vivo, the LNCaP CRPC xenograft model was used. All EPI analogs significantly inhibited CRPC tumor growth compared with DMSO control (Figure 2E). Consistent with in vitro responses, EPI-002 as well as EPI-005 had better antitumor activity compared with EPI-003 and EPI-004 (Figure 2F). EPI-002 and EPI-005 both have the S configuration for the chlorohydrin, whereas EPI-003 and EPI-004 have the R configuration. Tumor regression was attained in 60% of animals treated with EPI-002 and EPI-005, although EPI-002 caused greater regression and was superior to that achieved with bicalutamide (Figure 2G). The 10-mg/kg daily oral dose of bicalutamide has been previously shown to be effective in LNCaP xenografts (37). No significant loss of body weight was measured in animals treated with EPI-002, in contrast to EPI-005 and the other stereoisomers (Figure 2H). This difference in effect on body weight was the criteria for focusing on EPI-002 rather than EPI-005 in subsequent studies.

In vitro, EPI-001 blocks transcription of androgen-regulated genes in response to R1881 (21). Levels of expression of these genes were examined using xenografts from castrated hosts treated for 14 days with EPI-001, EPI-002, and bicalutamide. Under castrated conditions, no significant changes in levels of full-length *AR*, *PSA* (also known as *KLK3*), *KLK2*, and *FKBP5* transcripts were observed in xenografts treated with EPI-001 and EPI-002 compared with DMSO in castrated hosts (Figure 2I and Supplemental Figure 2). However, levels of *NKX3.1* and *TMPRSS2* transcripts were significantly decreased with EPI-001 and EPI-002 (Figure 2I). *RHOU*, *SLC41A1*, *GOLPH3*, and *PAK1IP1* were all significantly decreased with both bicalutamide and EPI-002, but not with EPI-001 (Supplemental Figure 2).

EPI chlorohydrin analogs covalently and specifically bind AR in living cells. EPI compounds that have a chlorohydrin group are active while those analogs that lack the chlorohydrin such as BADGE.2H_2O are inactive (21). The chlorohydrin group of EPI compounds may be required for activity to block AR transcriptional activity, and its chemical structure suggests a possible mechanism of covalent binding. To elucidate the mechanism of binding of EPI compounds to the AR and potentially other cellular proteins, cells were incubated with modified EPI probes containing an alkyne group to allow for Click-chemistry to add biotin to the EPI probe, followed by SDS-PAGE and Western blot analysis (Figure 3A). Whereas modified EPI probes containing the chlorohydrin group (Figure 3B) were active in cells and inhibited AR activity, EPI compounds lacking the chlorohydrin had relatively poor activity (Supplemental Figure 3 and Supplemental Table 3). LNCaP cells were exposed to EPI probes for 24 hours before lysing and Click-chemistry. Nonchlorinated EPI-051 and EPI-063 were negative controls, by analogy with the inactive analog BADGE.2H_2O (21). SDS-PAGE disrupts noncovalent interactions and is used to determine covalent binding. Western blot analysis using an antibody against biotin revealed a band corresponding to AR that was specific to EPI-046– and EPI-047–treated samples and was not present in the whole cell lysates of cells treated with DMSO or the inactive analog EPI-051 that lacks the chlorohydrin (Figure 3C, left, red outline). Lack of biotin bands detected in DMSO-treated and EPI-051–treated cells were not due to nondetectable levels of AR, as shown when the membrane was reprobed with an antibody against AR (Figure 3C, middle). EPI probes with the chlorohydrin, such as EPI-054 — closest to the structure of EPI-002 — did not bind an abundance of other cellular proteins (Figure 3D, top). Only 3 bands between 200 and 75 kDa were detected using an antibody to biotin that were unique to EPI-054 treatment compared with DMSO. Confirmation that the protein band at 110 kDa corresponded to AR was shown by detection of AR pulled down from streptavidin beads only in lanes treated with EPI-054, not from DMSO-treated cells (Figure 3D, bottom). Together, these data support the notion that the biotinylated band detected at 110 kDa with EPI-054 treatment corresponded to AR. All EPI probes with a chlorohydrin, regardless of chirality, bound covalently to full-length AR (FL-AR), while the nonchlorinated analogs did not (Figure 3E). Confirmation that chlorinated EPI probes interacted with the NTD was obtained using cells transfected with FLAG-tagged chimera of AR NTD (Figure 3F). Together, these data support that EPI analogs containing a chlorohydrin covalently bind to AR NTD in cells.

Chemical mechanism of EPI binding to AR AF1. As demonstrated above, EPI analogs with a chlorohydrin covalently bound to AR in cells. To further elucidate the chemical mechanism of binding, EPI-054 (chlorohydrin) or inactive EPI-063 (no chlorohydrin) was incubated with purified recombinant AF1 protein under cell-free conditions prior to Click-chemistry to add fluorescein to the EPI probe, followed by SDS-PAGE and detection of the fluorescent band corresponding to AF1 protein. The ratio of AR AF1 protein to EPI analog was examined as well as binding time. After 1 and 20 hours of binding reaction, EPI-054 covalently bound to AF1 in a dose-dependent manner, in contrast to EPI-063 (Figure 4A).

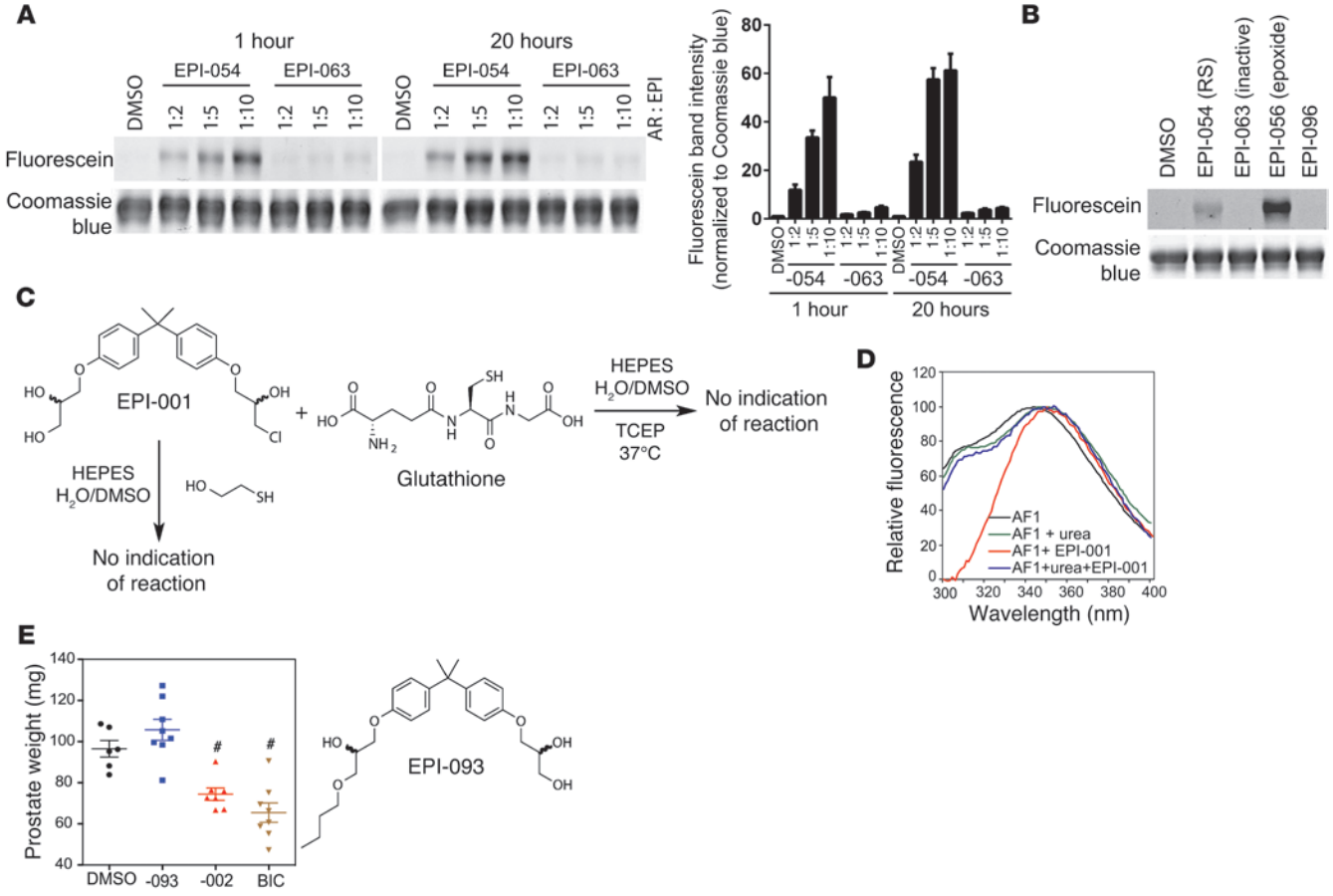

Figure 4

Chemical mechanism of EPI binding to AF1. (**A**) AF1 protein was incubated with EPI-054, EPI-063 (inactive), or DMSO (vehicle) at the indicated molar ratios on ice for 1 hour or 20 hours, prior to Click-chemistry for fluorescein labeling, SDS-PAGE, and detection of fluorescein-labeled probe covalently bound to AF1. Quantification of fluorescein band intensity, normalized to Coomassie blue bands, is also shown. The value from each EPI condition was normalized to the value of DMSO for each individual experiment (n = 4 separate experiments). (**B**) AF1 protein was incubated with DMSO, EPI-054, EPI-063, EPI-056, or EPI-096 (AF1/EPI 1:3 molar ratio) at 25°C for 18 hours, prior to Click-chemistry for fluorescein labeling, SDS-PAGE, and detection of fluorescein-labeled probe covalently bound to AF1. (**C**) EPI analogs do not alkylate glutathione or mercaptoethanol. A mixture of glutathione (127 μM) and EPI-001 (25 μM), or a mixture of EPI-001 (55 μM) and 2-mercaptoethanol (155 μM), was monitored by proton and carbon NMR over a period of 7 days. There was no evidence for reaction of EPI-001 with either glutathione or mercaptoethanol. (**D**) Steady-state spectra of 1 μM recombinant wild-type AF1 protein in buffer, buffer plus 2.9 μM EPI-001, buffer plus 6 M urea, or buffer plus 6 M urea and 2.9 μM EPI-001. (**E**) Prostate weights from mice treated with DMSO (i.v.), EPI-093 or EPI-002 (50 mg/kg body weight; i.v.), or bicalutamide (10 mg/kg body weight; gavage daily) for 14 days. Data are mean ± SEM. There was no significant difference between EPI and bicalutamide. $^{\#}P < 0.001$.

Quantification of the fluorescein/AF1 complex normalized to the corresponding coomassie blue band for each lane is also shown graphically from 4 separate experiments. After 20 hours, the binding reaction with EPI-054 was not significantly increased with a 1:10 AF1/EPI-054 ratio compared with the binding achieved with a 1:5 ratio. Even after 20 hours, the amount of covalent binding was relatively low compared with the total amount of AF1 protein available in each lane.

EPI-054, which has the same absolute configuration as EPI-002, contains the chlorohydrin substructure found in EPI-001 and its stereoisomers. EPI-063 is a mixture of stereoisomers that are simply missing the primary chloride that is present in EPI-001. EPI-096 is missing the secondary alcohol component of the chlorohydrin that is present in the EPI-001 stereoisomers, and EPI-056 has the chlorohydrin converted to an epoxide (Figure 3B). Importantly, although EPI-054 bound covalently to the AF1 protein, the reaction was slow and never reached completion during the experiment exposure times, whereas the epoxide containing probe EPI-056 reacted quickly and gave a much higher yield of covalent adduct (Figure 4B). Thus, EPI-054 bound covalently, and neither EPI-063 (which is simply missing the chloride functionality) nor EPI-096 (which is simply missing the secondary alcohol) bound covalently, to the AF1 protein (Figure 4B). These results demonstrate that the entire chlorohydrin substructure in the EPI-001 series was required for covalent binding, while a simple primary chloride, as found in EPI-096, was not sufficient. EPI analogs with chlorohydrins were not random alkylating agents, as shown by the lack of adducts when incubated with glutathione or mercaptoethanol (Figure 4C).

AR AF1 is intrinsically disordered, with approximately only 16% predicted α-helix secondary structure (27). To determine

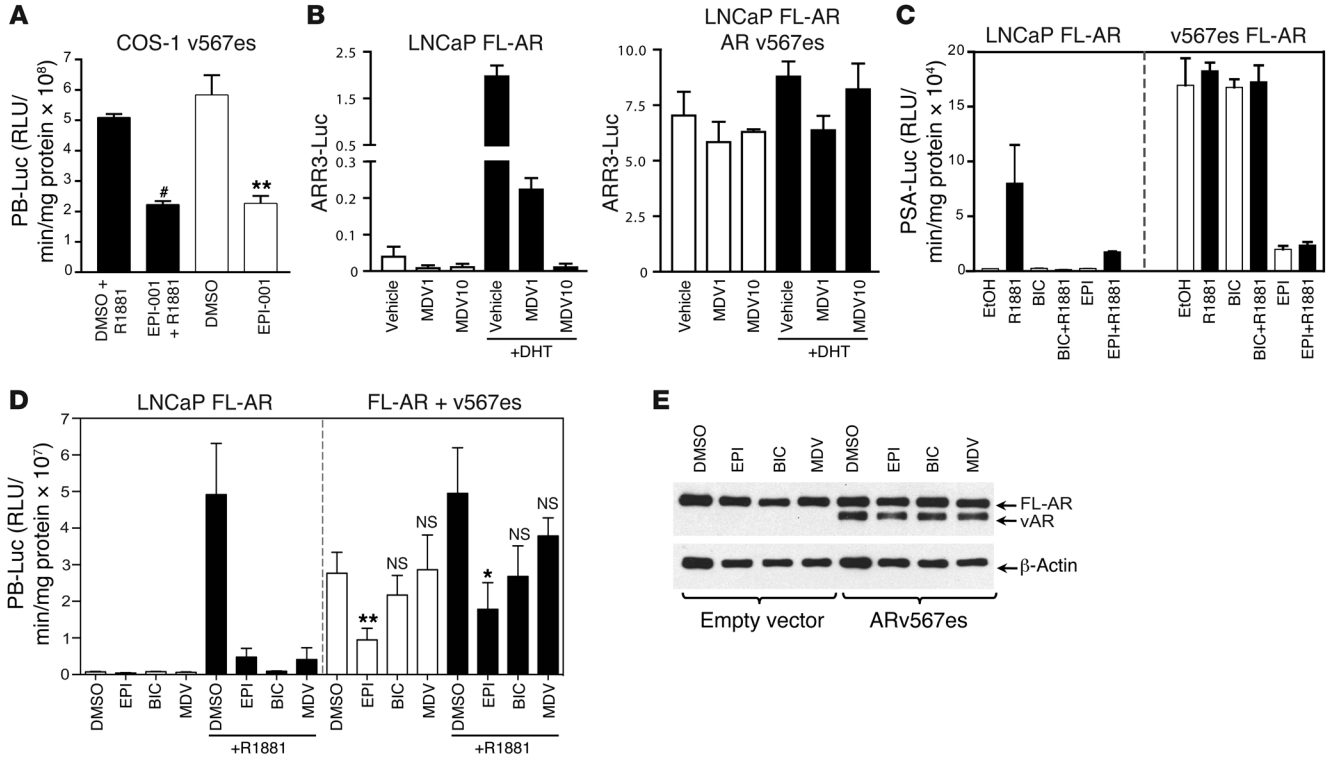

Figure 5

EPI inhibits splice variant AR^{v567es}. (**A**) COS-1 cells were transfected with PB-luciferase reporter and the AR^{v567es} variant and treated with DMSO or 25 μM EPI-001 plus 1 nM R1881 for 24 hours. (**B**) ARR3-luciferase activity in LNCaP cells with endogenous FL-AR (left) or with both FL-AR and AR^{v567es} (right), with or without MDV3100 (1 or 10 μM). (**C**) PSA(6.1kb)-luciferase activity in LNCaP cells with endogenous FL-AR (left) or with both FL-AR and AR^{v567es} (right). Cells were treated with DMSO, 25 μM EPI-001, or 10 μM bicalutamide with or without 1 nM R1881 for 48 hours. (**D**) PB-luciferase activity in LNCaP cells with endogenous FL-AR (left) or with both FL-AR and AR^{v567es} (right). Cells were treated with 25 μM EPI-001, 10 μM bicalutamide, and 5 μM MDV3100 for 1 hour prior to treatment with 1 nM R1881 for 24 hours. (**E**) Protein levels of FL-AR and AR^{v567es} from samples in **D**, detected using AR-N20 antibody. Data are mean ± SEM (**A** and **B**) or mean ± SD (**C** and **D**). n = 3 separate experiments. $^{*}P < 0.05$; $^{**}P < 0.01$; $^{\#}P < 0.001$.

whether EPI can bind to denatured AF1 protein or whether EPI requires the limited secondary structure for binding, the putative helical regions within AF1 were disrupted using urea, and changes in conformation of the AF1 protein were measured by steady-state fluorescence, which could be altered by both reversible and irreversible interaction with EPI-001. The steady-state fluorescence spectrum of AF1 denatured by urea showed a distinct peak for tyrosine and red shift for tryptophan (i.e., 343 nm to 350 nm), indicative of the tryptophan becoming more solvent exposed and the polypeptide being unstructured (28). Consistent with a requirement for some structure in the AF1 protein in order for EPI to bind, EPI-001 failed to bind to denatured AF1 protein to alter the steady-state spectrum. Instead, this spectrum of EPI with denatured AF1 was similar to the AF1 spectrum in urea without EPI-001, with a λ_{max} for tryptophan of 349 nm and a distinct peak for the tyrosine emission (Figure 4D). These results suggest that some secondary structure of AF1 is necessary for EPI-001 to bind. Finally, to provide an indication of whether the chlorohydrin group of EPI analogs may be necessary for in vivo activity, loss of weight of androgen-dependent tissue in mature male mice was examined, since this is the gold standard for on-target activity of drugs targeting the AR. Consistent with the requirement of a chlorohydrin and covalent binding for in vivo activity, only EPI-002 caused a significant reduction in prostate weight compared with DMSO control, similar to the reduction seen with bicalutamide, whereas EPI-093 had no significant effect (Figure 4E).

EPI inhibits constitutively active AR splice variants. Constitutively active AR splice variants that lack LBD have been shown in clinical samples of CRPC (16–19, 38). Antiandrogens that bind the AR LBD do not inhibit the activity of AR^{v567es}, which lacks LBD and is constitutively both nuclear and active (17). Variant AR^{v567es} is solely expressed in 20% of metastases and coexpressed with FL-AR in approximately 60% of CRPC metastases (17). Expression of AR^{v567es} in COS-1 cells, which lack endogenous AR, resulted in elevated PB-luciferase activity that was not altered by R1881, as previously reported (17). EPI-001 effectively attenuated AR^{v567es} activity (Figure 5A). A mixed population of FL-AR with AR^{v567es} was next examined in LNCaP cells. In the absence of AR^{v567es}, MDV3100 at both 1 and 10 μM inhibited FL-AR induced by androgen, as measured with ARR3-luciferase reporter (Figure 5B, left). However, MDV3100 had no effect in blocking AR activity, either in the presence or absence of androgen, when AR^{v567es} was introduced into LNCaP cells (Figure 5B, right). Consistent with the results obtained with MDV3100 using ARR3-luciferase reporter in the presence of AR^{V567es}, bicalutamide also had no

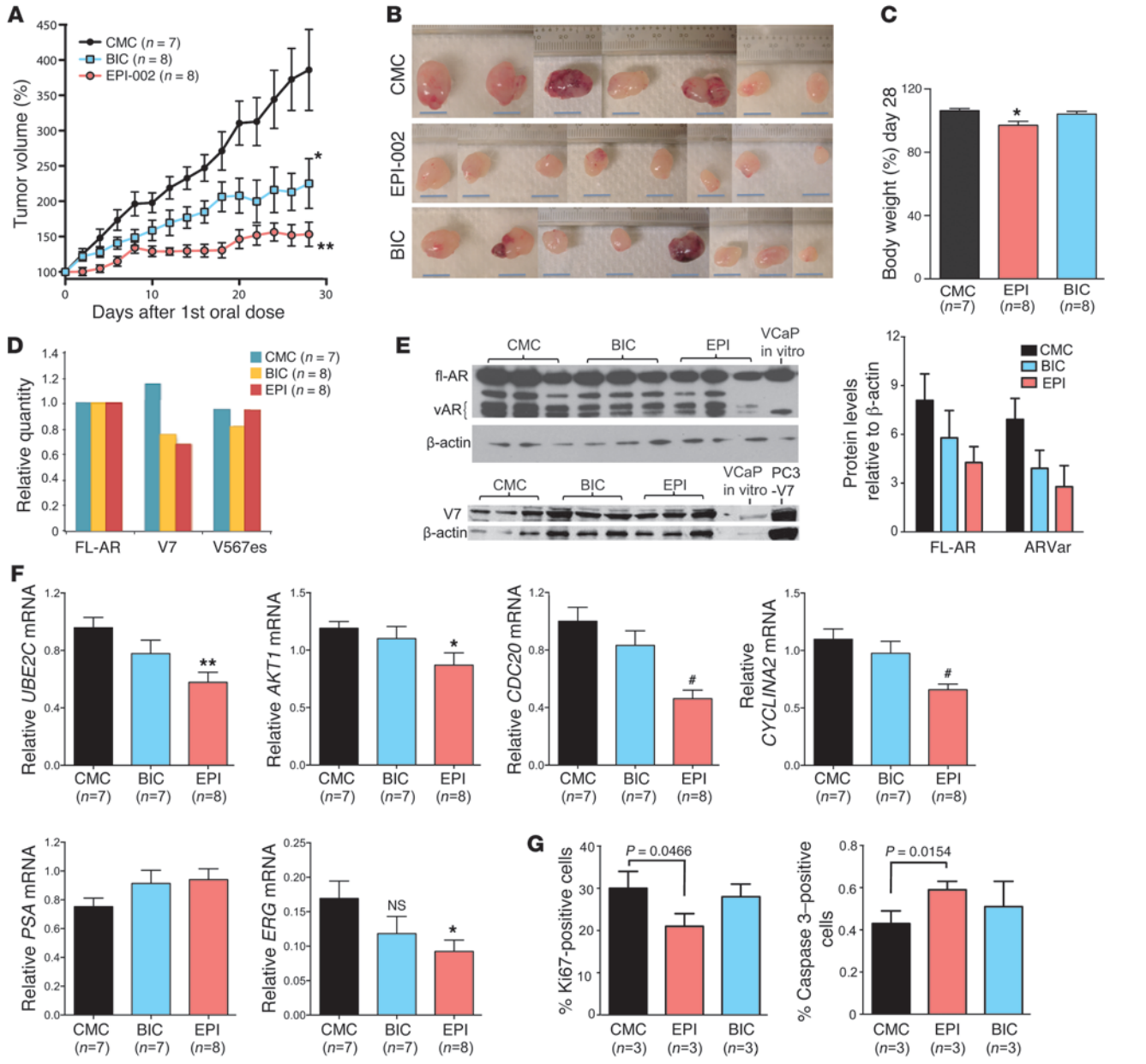

Figure 6

Oral dosing of EPI-002 blocks AR transcriptional program and inhibits growth of VCaP CRPC xenografts that express AR splice variants. (**A**) VCaP tumor growth in castrated mice administered EPI-002 (200 mg/kg body weight) or bicalutamide (10 mg/kg body weight) daily by gavage for a total of 28 doses. Tumors were harvested 2 days after the last treatment. (**B**) Photographs of tumors harvested at day 28 from animals as in **A**. Scale bars: 10 mm. (**C**) Body weight change over the duration of the experiment. (**D**) Transcript levels of FL-AR and AR variants (V7, V567es) normalized to *RPL13A* using total RNA isolated from VCaP xenografts from castrated hosts treated with bicalutamide ($n = 8$), EPI-002 ($n = 8$), or DMSO control (CMC; $n = 7$) for 28 days. (**E**) Protein levels of AR and AR variants from harvested xenografts treated with EPI-002 or bicalutamide or vehicle control. Quantification of protein bands (FL-AR and AR variant), normalized to β-actin, is also shown. (**F**) Transcript levels of *UBE2C*, *AKT1*, *CDC20*, *CYCLINA2*, *PSA*, and *ERG*, normalized to levels of *RPL13A*. (**G**) Proliferation (Ki67) and apoptosis (caspase-3) index, measured in harvested VCaP xenografts. Data are mean ± SEM. $^{*}P < 0.05$; $^{**}P < 0.01$; $^{\#}P < 0.001$.

effect on AR activity in LNCaP cells expressing both FL-AR and variant AR^{v567es}, as measured with PSA(6.1kb)-luciferase reporter. EPI-001 showed good activity against FL-AR as well as mixed populations of FL-AR with variant AR^{v567es} (Figure 5C). Thus, unlike the antiandrogens MDV3100 and bicalutamide, EPI inhibited FL-AR, AR^{v567es}, and mixtures of FL-AR and AR^{v567es}. Direct comparison of EPI, bicalutamide, and MDV3100 on solely endogenous FL-AR or endogenous FL-AR combined with AR^{v567es} using the PB-luciferase reporter in LNCaP cells in the presence and absence of androgen additionally confirmed the efficacy of EPI to significantly inhibit AR activity under conditions in which bicalutamide and MDV3100 failed to have any significant effect (Figure 5D).

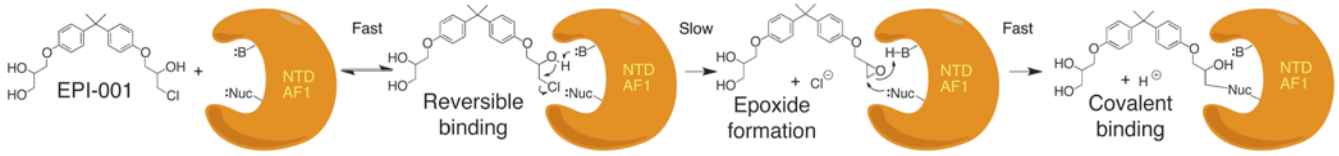

Figure 7
Covalent binding reaction of EPI compounds to AR AF1 region. First, there is a fast reversible interaction between EPI-001 and the AR AF1 region that places the secondary alcohol of the chlorohydrin functionality next to a basic site in AF1. Then, in a slow rate-determining step, the base removes the proton from the secondary alcohol to form an intermediate epoxide. The reactive epoxide reacts rapidly and irreversibly with a nucleophilic site on an amino acid side chain to form a covalent bond.

Western blot analysis using an antibody against the AR NTD confirmed the approximate 1:1 ratio of FL-AR to AR^{v567es} in whole cell lysates of LNCaP cells treated with EPI, MDV3100, and bicalutamide (Figure 5E). Thus, EPI analogs are the first reported inhibitors of constitutively active AR splice variants.

EPI-002 inhibits the growth of CRPC xenografts that express AR splice variants. The effect of EPI-002 on CRPC that express AR variants and FL-AR was investigated using VCaP xenografts and oral dosing in castrated hosts. VCaP cells exhibited amplified FL-AR and expressed AR variant within 14 days after castration. Pharmacokinetic studies indicated that EPI-001 had 86% bioavailability, a half-life of approximately 3.3 hours, and a slow clearance rate of 1.75 l/h/kg; moreover, blood levels of 10 μg/ml (25 μM) were achieved, which was the effective concentration in vitro (Supplemental Figure 4 and Supplemental Table 4). VCaP tumor volume in animals treated with EPI-002 was significantly less than the control and bicalutamide-treated groups (Figure 6, A and B). Animals treated daily for 28 days showed no changes in behavior and only minor body weight loss (Figure 6C). Weight loss with EPI-002 may be associated with frequent (twice daily) gavage and/or slight toxicity.

Contrary to abiraterone and MDV3100, which increase levels of both FL-AR and variant ARs (35, 38), EPI-002 did not increase either transcript or protein levels of FL-AR and splice variant ARs in harvested tumors (Figure 6, D and E). The transcriptional program associated with expression of AR variant was blocked in vivo by EPI-002, as supported by significantly decreased levels of *UBE2C*, *AKT1*, *CDC20*, and *CYCLINA2* transcripts in harvested tumors (Figure 6F). AR selectively upregulates expression of these M-phase cell cycle genes in CRPC (39), and their expression is associated with increased levels of AR variant in CRPC bone metastases (19). Bicalutamide inhibited FL-AR and had no effect on AR splice variants lacking LBD, and thus had no significant effect on the transcript levels of these M-phase genes (Figure 6F). Expression of genes regulated by FL-AR revealed that after castration and 28 days of treatment, neither bicalutamide nor EPI-002 had any significant effects on *PSA*, *TMPRSS2-ERG*, or *FKPB5* transcripts compared with DMSO (Figure 6F and data not shown). *ERG* transcript levels were significantly decreased with EPI-002, whereas bicalutamide did not achieve statistical significance (Figure 6F). Consistent with EPI-002 decreasing tumor volume and having an inhibitory effect on expression of M-phase genes associated with variant AR and CRPC, EPI-002 also significantly decreased proliferation and increased apoptosis, whereas bicalutamide had no significant effect, as determined by immunohistochemistry of sections of xenografts stained for Ki67 or caspase-3 (Figure 6G and Supplemental Figure 5).

Discussion

AR NTD is a unique therapeutic target for CRPC and potentially other diseases of the androgen axis. Functional NTD is necessary for AR transcriptional activity (23–25). The small molecule EPI-001 is a mixture of 4 stereoisomers that inhibits protein-protein interactions with CBP and RAP74 (21) that are required for AR transcriptional activity (26, 32). Here, our preclinical study of EPI-001 revealed (a) no stereospecificity in binding of stereoisomers to AR, although both in vitro and in vivo, the single stereoisomer EPI-002 (2R, 20S) had improved properties compared with other stereoisomers; (b) the chlorohydrin was required for covalent binding of EPI analogs to AF1 in the AR NTD; (c) EPI covalent binding was specific for AR; (d) EPI-001 did not bind to denatured AF1; (e) EPI-001 and EPI-002 inhibited a constitutively active AR splice variant that lacks LBD; (f) oral delivery of EPI-002 reduced the growth of CRPC xenografts expressing the AR variant; and (g) AR transcriptional program was blocked in vivo by EPI-002. The lead compound EPI-002 showed that AR NTD could be blocked, with a detrimental effect on CRPC. These findings revealed that small-molecule inhibitors can be developed against IDPs, such as the AR NTD, with excellent in vivo pharmacokinetics, efficacy, and specificity.

In vitro, stereoisomers with 20S chlorohydrin (EPI-002 and EPI-005) were significantly better in blocking AR transcriptional activity, depending on the reporter gene construct, than the 20R stereoisomers. Reporter specificity potentially involves recruitment of different binding partners to AR on androgen response elements (AREs). Since EPI inhibits protein-protein interactions, together, these data indicate that some androgen-regulated genes may have more sensitivity to EPI stereoisomer configuration. In vivo, stereoisomer EPI-002 had superior antitumor activity compared with the other stereoisomers and the EPI-001 mixture, which may reflect potential differences in EPI stereoisomers on the transcriptional program. This notion is supported by the finding that EPI-002 achieved statistical significance for decreasing *RHOU*, *SLC41A1*, *GOLPH3*, and *PAK1IP1*, whereas the EPI-001 mixture did not, although differences in pharmacokinetic properties may also be involved. AR-regulated gene expression substantially differs between VCaP and LNCaP cells in vitro in response to androgen and AR silencing (40). This may be due to the fact that VCaP cells have 5 extra copies of the AR gene (41) and 11-fold more *AR* mRNA than LNCaP cells (40); that VCaP cells express AR variants that have unique transcriptomes, while parental LNCaP cells do not express variant, but have a mutated AR and cell-specific differences in coregulators and signaling pathways; or that VCaP cells express the AR-regulated TMPRSS2-ERG fusion (42); or it may be due to differences in cellular/intratumoral levels of androgen. Differences observed here between gene expression

profiles in VCaP and LNCaP xenografts from castrated hosts in response to bicalutamide and EPI may also involve the different times of analysis after castration and drug treatment. LNCaP xenografts were harvested from hosts 21 days after castration and 14 days of drug treatment, while VCaP xenografts were harvested 35 days after castration and 28 days of treatment. Levels of *PSA* were not further decreased after castration by EPI compounds in either xenograft, whereas bicalutamide had an effect in LNCaP, but not VCaP, xenografts. *PSA* mRNA is not a sensitive marker of AR action (40), nor have *PSA* mRNA levels proved reliable as a prognostic marker for prostate cancer (43), in spite of serum levels of PSA being one of the best biomarkers used in oncology. Instead, 2 other well-characterized AR-regulated genes, *NKX3.1* and *TMPRSS2*, were significantly decreased by EPI in LNCaP xenografts from castrated hosts. Importantly, EPI-002 decreased transcript expression of the M-phase cell cycle genes *UBE2C*, *AKT1*, *CDC20*, and *CYCLINA2*, which are increased in CRPC and regulated by AR variant (39), in VCaP xenografts.

It is important to note that all stereoisomers covalently bound to the endogenous AR in cells. To our knowledge, these studies are the first to show binding of the different stereoisomers to an IDP in living cells; others have relied on functional assays or used recombinant proteins. The plasticity of IDPs that permits these proteins to bind multiple partners with an induced fit may result in less dependence on stereospecific properties, compared with structured proteins with rigid clefts and pockets. Thus, the demonstrated lack of stereospecific properties of the EPI analogs for binding to AR may reflect a malleable binding surface or large region for interaction on the AR NTD; alternatively, such lack of stereospecific properties may be a reflection of the potential flexible structure of the EPI compounds. The high-specificity and low-affinity interactions that are essential for reversible binding of multiple proteins to IDPs support that covalent binding of a small molecule may be optimal for sustained binding and therapeutic response. In support of this hypothesis, the noncovalent binding EPI analog EPI-093, which lacks the chlorohydrin, had no in vivo effects on the androgen axis, whereas the covalent binder EPI-002 decreased the weight of androgen-dependent tissue. The EPI compounds were not general alkylating agents, as indicated by the inability of EPI-001 to form adducts with glutathione and mercaptoethanol and from Click-chemistry experiments in living cells showing that EPI probes did not bind an abundance of cellular proteins.

Based on the evidence in Figures 3 and 4, we propose the following model of the chemical mechanism for the selective covalent of EPI-001 analogs to the AR NTD. First, the AR AF1 requires some secondary structure, since EPI compounds did not bind the denatured protein (Figure 4D). Then, the initial binding step possibly involves a fast reversible interaction between EPI-001 and the AR AF1 region (Figure 7). This reversible binding potentially situates the secondary alcohol of the chlorohydrin functionality adjacent to a basic site in AF1. In a slow and essentially irreversible step, the base might remove the proton from the secondary alcohol, leading to formation of an intermediate epoxide. The epoxide could then react with an adjacent nucleophilic site on an amino acid side chain (e.g., -SH [cysteine], -NH_2 [lysine, ornithine], phenoxide [tyrosine], or imidazole [histidine]) to form the covalent bond. The selectivity of this covalent binding may come from a combination of a requirement for a strong reversible binding interaction with AR AF1 and the necessity of having a basic functionality located adjacent to the chlorohydrin secondary alcohol in this reversibly bound EPI-001 that can form the reactive epoxide. The slow rate of covalent binding of EPI-054 compared with the epoxide EPI-056 may reflect the slow rate of conversion of the chlorohydrin EPI-054 to the epoxide EPI-056 on the AF1.

Approximately 40 drugs that are covalent binders have been approved by the FDA, including clopidogrel, lansoprazole, esomeprazole, abiraterone, aspirin, and therapeutics for long-term use (44). However, EPI is the first reported covalent binder to an IDP and is in clinical development for human studies. EPI analogs overcome some of the limitations of current therapies for CRPC, including EPI's low propensity for developing gain-of-function mutations because of the intrinsic disorder of the NTD and covalent binding. Importantly, EPI analogs are the only known inhibitors of constitutively active AR splice variants that are correlated to CRPC, poor prognosis, and resistance to abiraterone (16–19, 35, 38). This paradigm for drug development could be applied to other IDPs that are associated with cancer and other diseases.

Methods

Cells, plasmids, and reporter assays. LNCaP, PC3, and VCaP cells as well as PSA(6.1kb)-luciferase, PB-luciferase, ARR3-luciferase, 5xGAl4UAS-TATA–luciferase, AR_{1-558}-Gal4DBD, AR^{v567es} plasmids, and transfection of cells have been described previously (17, 21).

Fluorescence polarization, microscopy, and spectroscopy. Androgen, progesterone, and glucocorticoid receptor PolarScreen Competitor Assay kits (Invitrogen) were used according to the manufacturer's protocol. Serial dilution was done for each small molecule, and solvent was compensated to ensure equal volume of DMSO and ethanol in each sample. Fluorescence polarization at excitation wavelength 470 nm and emission at 530 nm were measured in Greiner 384 black clear-bottomed plates using Infinite M1000 (TECAN).

For microscopy, LNCaP cells were transiently transfected with an expression vector for AR-YFP using serum-free and phenol red–free RPMI media for 24 hours prior to treatment of compounds. 4 hours after treatment, cells were fixed and stained for DAPI and examined using fluorescence microscopy.

Steady-state fluorescence spectroscopy was measured as described previously (21, 28), and on-site competition curve best-fit analysis was performed using GraphPad Prism version 6.01 software.

BrdU cell cycle analysis. LNCaP cells were treated with inhibitors for 1 hour, followed by addition of 0.1 nM R1881 under serum-free and phenol red–free conditions for 48 hours. Cells were pulse labeled with 10 μM BrdU for 2 hours and fixed in 70% ethanol. BrdU-labeled cells were probed with anti-BrdU–FITC antibody, and DNA was counterstained with DAPI. List mode files were collected using a dual laser Epics Elite-ESP flow cytometer. Bivariate analysis was performed using FlowJo 7 software (Ashland).

Viability and proliferation assays. PC3 and LNCaP cells were plated in 96-well plates in respective media plus 0.5% FBS. The next day, PC3 cells were treated with vehicle and EPI-002 for 2 days, and LNCaP cells were pretreated with vehicle and EPI-002 for 1 hour before treating with 0.1 nM R1881 for 3 days. Cell viability was measured using alamarBlue Cell Viability Assay (Invitrogen) following the manufacturer's protocol.

Binding assays. LNCaP cells were treated for 24 hours with vehicle or with alkyne-containing EPI analogs. To examine binding to the AR NTD, LNCaP cells were transiently transfected with Flag-ARN plasmid or empty vector using lipofectin (Invitrogen) and treated with vehicle or modified EPI-001 analogs for 24 hours. Proteins were extracted from treated cells with lysis buffer containing 50 mM HEPES (pH 8.0), 150 mM NaCl, 1% (v/v) Triton-X100, and EDTA-free protease inhibitors and were subjected to Click-chemistry conditions for 3 hours at 25°C in buffer containing 0.1% SDS,

5% t-butanol, 100 μM tris[(1-benzyl-1H-1,2,3-triazol-4-yl)methyl]amine (Sigma-Aldrich), 1 mM tris-(2-carboxyethyl) phosphine (TCEP), 100 μM biotin-azide reagent, and 1 mM $CuSO_4$. Samples were dialyzed overnight in 50 mM HEPES (pH 8.0), 150 mM NaCl, 0.1% SDS, and 1% Triton-X100 to remove excess biotin-azide reagent. Biotinylated EPI probes covalently bound to proteins were enriched using streptavidin-agarose resin (Thermo Fisher Scientific). Biotin-EPI-proteins were separated by SDS-PAGE and subjected to Western blot analysis using anti-biotin antibody.

The cell-free binding assay was performed with AR AF1 recombinant protein that was expressed and purified as previously described (21, 28), with additional purification by size exclusion chromatography. Recombinant AR AF1 was mixed with alkyne-containing EPI probes, and binding reaction was carried out under the conditions indicated in the figures and legends prior to heating (90°C for 5 minutes). EPI probes were labeled with fluorescein by Click-chemistry reaction at 25°C for 1 hour in buffer containing fluorescein azide (in amounts exceeding those of the EPI probes), 0.1 mM ascorbic acid, and 0.1 mM copper(II)-tris[(1-benzyl-1H-1,2,3-triazol-4-yl)methyl]amine complex (Lumiprobe). Samples were resolved on 12.5% SDS-PAGE, and fluorescein was visualized using Fujifilm FLA-7000 image analyzer (GE Healthcare). The same gel was stained with Coomassie blue R-250. The intensities of bands for fluorescein or Coomassie blue were quantified using ImageJ.

Alkylation reaction. Test solutions were prepared by placing 10 μg EPI-001 into a NMR tube in DMSO/HEPES buffer (4:1, v/v, 0.10 M HEPES, pH 7.4), adding thiols (neat liquid or solid form), and diluting the solution with 100 μl TCEP (0.5 M). The NMR spectra experiments were set to be monitored at 25°C at 0, 1, 3, 5, 7, and 24 hours as well as 7 days after the addition of thiols.

For glutathione screening, glutathione (39 mg, 0.127 mmol) and TCEP (100 μl) were added to a solution of EPI-001 (10 μg, 0.025 mmol) in DMSO-d_6/HEPES buffer (500 μl). After shaking several times, the reaction mixture was monitored by NMR.

For 2-mercaptoethanol screening, 2-mercaptoethanol (11 μl, 0.155 mmol) was added to a solution of EPI-001 (22 μg, 0.055 mmol) in DMSO-d_6. After shaking several times, the reaction mixture was monitored by NMR.

Prostate weight. Mature male mice were treated every 3 days with EPI-093 (i.v.), EPI-002 (i.v.), DMSO control (i.v.) or daily with bicalutamide (10 mg/kg body weight by gavage). 2 days after the last dose, prostates were dissected and weighed.

Xenografts. Male NOD-SCID mice bearing subcutaneous tumors were castrated when tumor volume was approximately 100 mm^3. Animals bearing LNCaP xenografts were injected i.v. with 50 mg/kg body weight of EPI-001 mixture or stereoisomers every other day or were treated by oral gavage with bicalutamide (10 mg/kg body weight). Animals bearing VCaP xenografts were administered 200 mg/kg body weight of EPI-002 (100-mg/kg dose twice daily), 10 mg/kg body weight of bicalutamide, or vehicle daily by oral gavage. Tumors were excised 2 days after the last dose and prepared for gene expression analysis, Western blot analyses, and immunohistochemistry.

QRT-PCR gene expression analysis. Total RNA was extracted from harvested xenografts using TRIzol reagent (Invitrogen) and PureLIink RNA Mini Kit (Invitrogen) according to the manufacturer's protocols specified for On-column PureLink DNase treatment. cDNA was subsequently synthesized using SuperScript III First-Strand Synthesis System for RT-PCR (Invitrogen). Diluted cDNA and gene-specific primers were mixed with Platinum SYBR Green qPCR SuperMix-UDG with ROX (Invitrogen). The transcripts were measured by ABI PRISM 7900 Sequence Detection System (Invitrogen). For all qRT-PCR experiments, each tumor sample was tested in technical triplicates. Gene expression levels were normalized to the housekeeping gene *RPL13A*. Primers were as previously described (21, 38).

Immunohistochemistry and Western blot analysis. Cells that were positive for Ki67 and caspase-3 staining were counted in sections from 3 xenografts per treatment. At least 2,000 cells per xenograft were counted. The total number of cells counted was as follows: 7,647 (DMSO, Ki67), 7,690 (EPI-002, Ki67), 7,901 (bicalutamide, Ki67), 8,799 (DMSO, caspase-3), 8,075 (EPI-002, caspase-3), and 7,843 (bicalutamide, caspase-3). For analysis of AR protein, concentrations of lysates of homogenized VCaP xenografts were measured by BCA assay after albumin depletion. Proteins (10 μg) were resolved on a NuPAGE 8%–12% Bis Tris gradient gel, transferred to nitrocellulose membrane, and probed for AR species using antibodies to the NTD (AR441; Santa Cruz). Protein levels of FL-AR and AR^{567} were detected using AR-N20 (Santa Cruz).

Statistics. Statistical analysis was performed using GraphPad Prism (version 6.01; GraphPad Software). Except where specified, comparisons between groups were performed with 2-tailed Student's *t* test, and differences were consider statistically significant at *P* values less than 0.05.

Study approval. All experiments involving animals conformed to the relevant regulatory and ethical standards, and the University of British Columbia Animal Care Committee approved the experiments.

Acknowledgments

This research was supported by grants from the NCI (2R01 CA105304), the Canadian Institutes of Health Research (MOP79308 and PPP90150), the Canadian Cancer Society (017289), the US Army Medical Research and Materiel Command Prostate Cancer Research Program (W81XWH-11-1-0551), NCI Pacific Northwest Prostate Cancer SPORE (2 P50 CA 097186-06 Project 4), PO1 CA85859, and the Department of Veterans Affairs to S. Plymate. We are grateful to Country Meadows Senior Men's Golf Charity Classic, the FORE PAR Prostate Awareness Research Charity Golf Classic, and Safeway for their financial support of this research.

Received for publication August 17, 2012, and accepted in revised form March 28, 2013.

Address correspondence to: Marianne D. Sadar, Genome Sciences Centre, BC Cancer Agency, 675 West 10th Avenue, Vancouver, British Columbia V5Z 1L3, Canada. Phone: 604.675.8157; Fax: 604.675.8178; E-mail: msadar@bcgsc.ca.

1. Uversky VN. Multitude of binding modes attainable by intrinsically disordered proteins: a portrait gallery of disorder-based complexes. *Chem Soc Rev*. 2011;40(3):1623–1634.
2. Sadar MD. Small molecule inhibitors targeting the "achilles' heel" of androgen receptor activity. *Cancer Res*. 2011;71(4):1208–1213.
3. Visakorpi T, et al. In vivo amplification of the androgen receptor gene and progression of human prostate cancer. *Nat Genet*. 1995;9(4):401–406.
4. Chen CD, et al. Molecular determinants of resistance to antiandrogen therapy. *Nat Med*. 2004;10(1):33–39.
5. Fenton MA, et al. Functional characterization of mutant androgen receptors from androgen-independent prostate cancer. *Clin Cancer Res*. 1997; 3(8):1383–1388.
6. Yoshida T, et al. Antiandrogen bicalutamide promotes tumor growth in a novel androgen-dependent prostate cancer xenograft model derived from a bicalutamide-treated patient. *Cancer Res*. 2005; 65(21):9611–9616.
7. Sadar MD. Androgen-independent induction of prostate-specific antigen gene expression via cross-talk between the androgen receptor and protein kinase A signal transduction pathways. *J Biol Chem*. 1999;274(12):7777–7783.
8. Ueda T, Bruchovsky N, Sadar MD. Activation of the androgen receptor N-terminal domain by interleukin-6 via MAPK and STAT3 signal transduction pathways. *J Biol Chem*. 2002;277(9):7076–7085.
9. Ueda T, Mawji NR, Bruchovsky N, Sadar MD. Ligand-independent activation of the androgen receptor by interleukin-6 and the role of steroid receptor coactivator-1 in prostate cancer cells. *J Biol Chem*. 2002;277(41):38087–38094.
10. Blaszczyk N, et al. Osteoblast-derived factors induce androgen-independent proliferation and expression of prostate-specific antigen in human prostate cancer cells. *Clin Cancer Res*. 2004;10(5):1860–1869.

11. Fujimoto N, Mizokami A, Harada S, Matsumoto T. Different expression of androgen receptor coactivators in human prostate. *Urology*. 2001;58(2):289–294.
12. Agoulnik IU, et al. Androgens modulate expression of transcription intermediary factor 2, an androgen receptor coactivator whose expression level correlates with early biochemical recurrence in prostate cancer. *Cancer Res*. 2006;66(21):10594–10602.
13. Comuzzi B, et al. The androgen receptor co-activator CBP is up-regulated following androgen withdrawal and is highly expressed in advanced prostate cancer. *J Pathol*. 2004;204(2):159–166.
14. Debes JD, et al. p300 in prostate cancer proliferation and progression. *Cancer Res*. 2003;63(22):7638–7640.
15. Montgomery RB, et al. Maintenance of intratumoral androgens in metastatic prostate cancer: a mechanism for castration-resistant tumor growth. *Cancer Res*. 2008;68(11):4447–4454.
16. Guo Z, et al. A novel androgen receptor splice variant is up-regulated during prostate cancer progression and promotes androgen depletion-resistant growth. *Cancer Res*. 2009;69(6):2305–2313.
17. Sun S, et al. Castration resistance in human prostate cancer is conferred by a frequently occurring androgen receptor splice variant. *J Clin Invest*. 2010; 120(8):2715–2730.
18. Hu R, et al. Ligand-independent androgen receptor variants derived from splicing of cryptic exons signify hormone-refractory prostate cancer. *Cancer Res*. 2009;69(1):16–22.
19. Hornberg E, et al. Expression of androgen receptor splice variants in prostate cancer bone metastases is associated with castration-resistance and short survival. *PLoS One*. 2011;6(4):e19059.
20. Quayle SN, Mawji NR, Wang J, Sadar MD. Androgen receptor decoy molecules block the growth of prostate cancer. *Proc Natl Acad Sci U S A*. 2007; 104(4):1331–1336.
21. Andersen RJ, et al. Regression of castrate-recurrent prostate cancer by a small-molecule inhibitor of the amino-terminus domain of the androgen receptor. *Cancer Cell*. 2010;17(6):535–546.
22. Heemers HV, Tindall DJ. Androgen receptor (AR) coregulators: a diversity of functions converging on and regulating the AR transcriptional complex. *Endocr Rev*. 2007;28(7):778–808.
23. Jenster G, et al. Domains of the human androgen receptor involved in steroid binding, transcriptional activation, and subcellular localization. *Mol Endocrinol*. 1991;5(10):1396–1404.
24. Simental JA, Sar M, Lane MV, French FS, Wilson EM. Transcriptional activation and nuclear targeting signals of the human androgen receptor. *J Biol Chem*. 1991;266(1):510–518.
25. Rundlett SE, Wu XP, Miesfeld RL. Functional characterizations of the androgen receptor confirm that the molecular basis of androgen action is transcriptional regulation. *Mol Endocrinol*. 1990;4(5):708–714.
26. McEwan IJ, Gustafsson J. Interaction of the human androgen receptor transactivation function with the general transcription factor TFIIF. *Proc Natl Acad Sci U S A*. 1997;94(16):8485–8490.
27. Lavery DN, McEwan IJ. Structural characterization of the native NH2-terminal transactivation domain of the human androgen receptor: a collapsed disordered conformation underlies structural plasticity and protein-induced folding. *Biochemistry*. 2008;47(11):3360–3369.
28. Reid J, Kelly SM, Watt K, Price NC, McEwan IJ. Conformational analysis of the androgen receptor amino-terminal domain involved in transactivation. Influence of structure-stabilizing solutes and protein-protein interactions. *J Biol Chem*. 2002; 277(22):20079–20086.
29. Fischer K, Kelly SM, Watt K, Price NC, McEwan IJ. Conformation of the mineralocorticoid receptor N-terminal domain: evidence for induced and stable structure. *Mol Endocrinol*. 2010;24(10):1935–1948.
30. Kumar R, Litwack G. Structural and functional relationships of the steroid hormone receptors' N-terminal transactivation domain. *Steroids*. 2009; 74(12):877–883.
31. Kumar R, Thompson EB. Transactivation functions of the N-terminal domains of nuclear hormone receptors: protein folding and coactivator interactions. *Mol Endocrinol*. 2003;17(1):1–10.
32. Aarnisalo P, Palvimo JJ, Janne OA. CREB-binding protein in androgen receptor-mediated signaling. *Proc Natl Acad Sci U S A*. 1998;95(5):2122–2127.
33. Bhalla J, Storchan GB, MacCarthy CM, Uversky VN, Tcherkasskaya O. Local flexibility in molecular function paradigm. *Mol Cell Proteomics*. 2006; 5(7):1212–1223.
34. Tran C, et al. Development of a second-generation antiandrogen for treatment of advanced prostate cancer. *Science*. 2009;324(5928):787–790.
35. Mostaghel EA, et al. Resistance to CYP17A1 inhibition with abiraterone in castration-resistant prostate cancer: induction of steroidogenesis and androgen receptor splice variants. *Clin Cancer Res*. 2011; 17(18):5913–5925.
36. Masiello D, Cheng S, Bubley GJ, Lu ML, Balk SP. Bicalutamide functions as an androgen receptor antagonist by assembly of a transcriptionally inactive receptor. *J Biol Chem*. 2002;277(29):26321–26326.
37. Clegg NJ, et al. ARN-509: a novel antiandrogen for prostate cancer treatment. *Cancer Res*. 2012; 72(6):1494–1503.
38. Zhang X, et al. Androgen receptor variants occur frequently in castration resistant prostate cancer metastases. *PLoS One*. 2011;6(11):e27970.
39. Wang Q, et al. Androgen receptor regulates a distinct transcription program in androgen-independent prostate cancer. *Cell*. 2009;138(2):245–256.
40. Makkonen H, Kauhanen M, Jaaskelainen T, Palvimo JJ. Androgen receptor amplification is reflected in the transcriptional responses of Vertebral-Cancer of the prostate cells. *Mol Cell Endocrinol*. 2011;331(1):57–65.
41. Liu W, et al. Homozygous deletions and recurrent amplifications implicate new genes involved in prostate cancer. *Neoplasia*. 2008;10(8):897–907.
42. Tomlins SA, et al. Distinct classes of chromosomal rearrangements create oncogenic ETS gene fusions in prostate cancer. *Nature*. 2007;448(7153):595–599.
43. Mostaghel EA, et al. Intraprostatic androgens and androgen-regulated gene expression persist after testosterone suppression: therapeutic implications for castration-resistant prostate cancer. *Cancer Res*. 2007;67(10):5033–5041.
44. Singh J, Petter RC, Baillie TA, Whitty A. The resurgence of covalent drugs. *Nat Rev Drug Discov*. 2011; 10(4):307–317.

Oncogene (2013), 1–11

www.nature.com/onc

ORIGINAL ARTICLE

Mechanisms of the androgen receptor splicing in prostate cancer cells

LL Liu[1], N Xie[1], S Sun[2], S Plymate[2], E Mostaghel[3] and X Dong[1,4]

Prostate tumors develop resistance to androgen deprivation therapy (ADT) by multiple mechanisms, one of which is to express constitutively active androgen receptor (AR) splice variants lacking the ligand-binding domain. AR splice variant 7 (AR-V7, also termed AR3) is the most abundantly expressed variant that drives prostate tumor progression under ADT conditions. However, the molecular mechanism by which AR-V7 is generated remains unclear. In this manuscript, we demonstrated that RNA splicing of AR-V7 in response to ADT was closely associated with *AR* gene transcription initiation and elongation rates. Enhanced *AR* gene transcription by ADT provides a prerequisite condition that further increases the interactions between AR pre-mRNA and splicing factors. Under ADT conditions, recruitment of several RNA splicing factors to the 3′ splicing site for AR-V7 was increased. We identified two RNA splicing enhancers and their binding proteins (U2AF65 and ASF/SF2) that had critical roles in splicing AR pre-mRNA into AR-V7. These data indicate that ADT-induced *AR* gene transcription rate and splicing factor recruitment to AR pre-mRNA contribute to the enhanced AR-V7 levels in prostate cancer cells.

Oncogene advance online publication, 15 July 2013; doi:10.1038/onc.2013.284

Keywords: prostate cancer; androgen deprivation therapy; RNA splice variant; alternative splicing

INTRODUCTION

The primary treatment for metastatic prostate cancer (PCa) is androgen deprivation therapy (ADT). Although initially effective, most tumors progress to castration-resistant PCa (CRPC) even under treatment with the most potent anti-androgens (for example, MDV3100 (enzalutamide) and abiraterone). No curative therapy is available.[1] It is commonly agreed that reactivation of the androgen receptor (AR) signaling contributes to CRPC[2,3] through several proposed mechanisms, including *AR* gene amplification/mutation and AR protein overexpression,[4,5] intratumoral androgen synthesis,[6,7] aberrant expression of AR co-regulators[8] and alternative AR activation by cytokines and growth factors in the absence of androgens.[9] In addition, recent findings indicate that the AR is also expressed as C-terminal-truncated variants, called ARvs, through alternative RNA splicing.[10–15] Lacking the ligand-binding domain of full-length AR (AR), ARvs are constitutively active in driving AR-regulated transcription and promoting tumor progression, even under castrate conditions.[11,13,15,16] ARvs regulate a mitotic form of the AR transcriptome rather than one associated with more differentiating functions.[17,18] Expression of ARvs occurs frequently in CRPC tumors.[19] Although a number of ARvs have been described in PCa cell lines and xenografts, AR splice variant 7 (AR-V7, also termed AR3) is the most commonly expressed ARv in human tissues.[11,13,20] Its levels are correlated with increased risk of biochemical relapse[11,13] and shorter survival time of CRPC patients.[20] These results suggest a critical role of AR-V7 in supporting CRPC. However, the molecular mechanism by which AR-V7 mRNA is spliced remains unclear.

Pre-mRNA splicing involves stepwise assembly of RNA splicing factors to the regions containing 5′ and 3′ splicing sites, excision of the intron sequences and re-ligation of the adjacent exons.[21] Alternative RNA splicing is the process whereby exons are selectively excised from the pre-mRNA, resulting in a different combination of exons in the final translated mRNA.[22] AR-V7 mRNA is spliced at the alternative 3′ splice site (3′ss) next to a cryptic exon, exon 3B, rather than the 3′ss next to exon 4, resulting in translation of a C-terminal-truncated form of the AR protein.[11,13] The decision as to which splicing site is excised is determined by both the regulatory RNA sequences (*cis* elements) and their associated RNA splicing proteins (*trans* elements). Depending upon the functional significance and location, some regulatory *cis* elements are termed exonic splicing enhancers (ESE) or intronic splicing enhancers (ISE).[23,24] In addition, RNA splicing is closely coupled with gene transcription.[25] Both transcription initiation[26] and elongation rates[27,28] have a significant impact on the outcome of splicing. This is achieved by the association of RNA splicing factors to the transcription machinery when transcription is initiated.[29–31] These protein complexes move along the gene during transcription elongation, when transcribed pre-mRNA is screened by the RNA spliceosome to define and excise the splice sites, before transcription is terminated.[32–34] Therefore, the abundance of a specific splice variant is controlled by both gene transcription rate and splicing factor recruitment to the pre-mRNA during the alternative splicing process.

The question that remains to be answered is whether ADT regulates the RNA splicing program that favors RNA synthesis of ARvs as a survival strategy for PCa in response to ADT. In this

[1]Department of Urologic Sciences, Vancouver Prostate Centre, University of British Columbia, Vancouver, British Columbia, Canada; [2]Department of Medicine, University of Washington School of Medicine and VAPSHCS-GRECC, Seattle, WA, USA; [3]Fred Hutchinson Cancer Research Center, Seattle, WA, USA and [4]Department of Obstetrics and Gynaecology, University of Toronto, Toronto, Ontario, Canada. Correspondence: Dr S Plymate, Department of Medicine, University of Washington School of Medicine and VAPSHCS-GRECC, Box 359625, 325 9th Avenue, Seattle 98104, WA, USA or Professor X Dong, Department of Urologic Sciences, The Vancouver Prostate Centre, University of British Columbia, 2660 Oak Street, Vancouver V6H 3Z6, British Columbia, Canada.
E-mail: splymate@u.washington.edu or xdong@prostatecentre.com
Received 24 February 2013; revised 12 June 2013; accepted 14 June 2013

manuscript, we studied the molecular mechanisms by which AR-V7 was alternatively spliced in response to ADT.

RESULTS

AR and AR-V7 mRNA levels are increased in response to androgen deprivation

We first profiled AR and AR-V7 RNA levels in a panel of PCa cell lines: VCaP, LNCaP, LN(AI) and LN95. Both LN(AI) and LN95 cells are derived from LNCaP cells, but have been cultured under long-term ADT conditions, thus possessing an ADT-resistant phenotype. Using an absolute quantification method, real-time quantitative PCR (qPCR) showed that VCaP cells expressed AR RNA that was 5–10 fold higher than LNCaP and LNCaP-derived cells (Figure 1 and Supplementary Figure 1A), which was consistent with the report that VCaP cells have an increased *AR* gene copy number.[35] AR RNA level was ~17.9-fold higher than AR-V7 in VCaP cells. LNCaP cells expressed extremely low levels of AR-V7 RNA. Both LN(AI) and LN95 cells expressed higher levels of AR-V7 than LNCaP cells. AR-V7 RNA levels in LN95 cells were 30–40% lower than that in VCaP cells. Western blotting assays showed consistently that VCaP cells expressed higher AR protein levels than other cell lines (Figure 1b and Supplementary Figure 1B), possibly due to the increase in *AR* gene copy number in VCaP cells. Both VCaP and LN95 cells expressed comparable levels of AR-V7 protein. LN(AI) cells expressed lower levels of AR-V7 protein, whereas parental LNCaP cells had undetectable levels of AR-V7 protein.

ADT conditions were reported to increase both RNA and protein levels of AR in PCa cell lines and xenografts.[17,36] To determine whether ADT also regulated AR-V7 expression, we treated PCa cells with dihydrotestosterone (DHT) and/or MDV3100 (Figure 1c). DHT reduced AR RNA levels significantly in VCaP and LNCaP cells, but only to a minor extent in LN(AI) cells. AR-V7 levels in LN(AI) cells were also repressed by DHT, following the changes of AR levels. In contrast, neither AR nor AR-V7 RNA levels were altered by DHT or MDV treatment in LN95 cells.

We found that AR-V7 expression was also reversibly regulated by DHT and MDV treatments. After VCaP cells were pre-treated with DHT for 24 h, adding MDV to the culture medium dramatically upregulated AR-V7 RNA and protein levels (Figure 2a–c). *Vice versa*, DHT significantly supressed AR-V7 expression after VCaP cells were pre-treated with MDV. Changes in AR-V7 RNA levels were correlated with AR levels. Using primary cultures from MDV-resistant VCaP tumor xenografts grown in mice ($n = 10$), we further showed that both AR and AR-V7 RNA levels were maintained in relative high levels under maximum ADT conditions, but significantly decreased when DHT was added (Figure 2d). As the doubling time of VCaP cells is 53 h, changes in AR and AR-V7 RNA levels cannot be accounted by clonal selection. These results indicated that RNA splicing of AR-V7 was a dynamic and reversible process, which was regulated by AR signaling.

AR-V7 expression is important for VCaP cell proliferation under ADT conditions

The functional significance of AR-V7 expression was further tested in VCaP cells by comparing cell proliferation rates under conditions of AR versus AR-V7 knockdown by small interfering RNA (siRNA). siRNA to exon 7 knocked down AR, siRNA to exon 3B knocked down AR-V7 and siRNA to exon 1 knocked down total AR (AR-V7 + AR). In the presence of androgen depletion and/or MDV treatments, AR-V7 or total AR, but not AR knockdown, significantly reduced VCaP cell growth (Figure 3a). However, cell growth relied

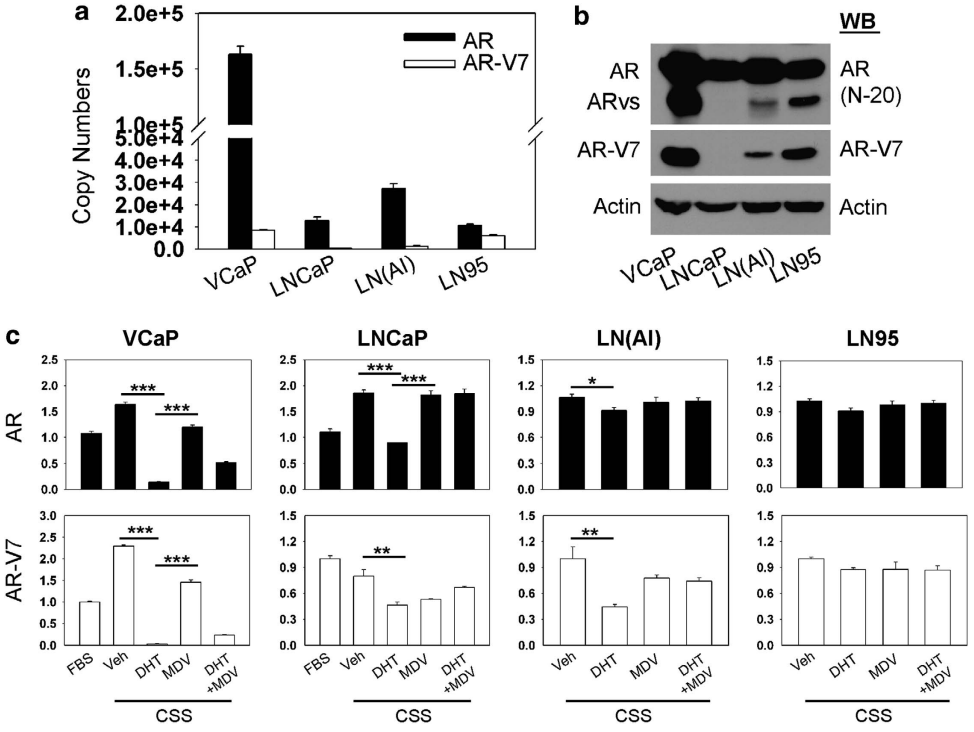

Figure 1. AR and AR-V7 RNA levels in PCa cells. (**a**) Total RNA was extracted from VCaP, LNCaP, LN(AI) and LN95 cells. AR and AR-V7 mRNA copy numbers within 20 ng RNA were determined by real-time qPCR using absolute quantification as described in Materials and methods. (**b**) AR and AR-V7 protein levels were detected by western blotting assays using AR(N-20) and AR-V7 antibodies. (**c**) VCaP, LNCaP, LN(AI) and LN95 cells were maintained in RPMI1640 medium containing 5% FBS or 5% CSS for 48 h. Cells were treated with vehicle (Veh), 10 nM DHT and/or 5 μM MDV3100 for 24 h. Relative RNA levels of AR and AR-V7 were determined by real-time qPCR using relative quantification to GAPDH. Results were obtained from three independent experiments with samples in triplicates and shown as mean ± s.e.m. One-way ANOVA followed by Student's *t*-test was carried out using GraphPad Prism showing significance with $P < 0.05$ as * or $P < 0.01$ as ** or $P < 0.001$ as ***. Primer sequences and standard curves for measuring RNA levels of AR and AR-V7 were presented in Supplementary Materials and figures.

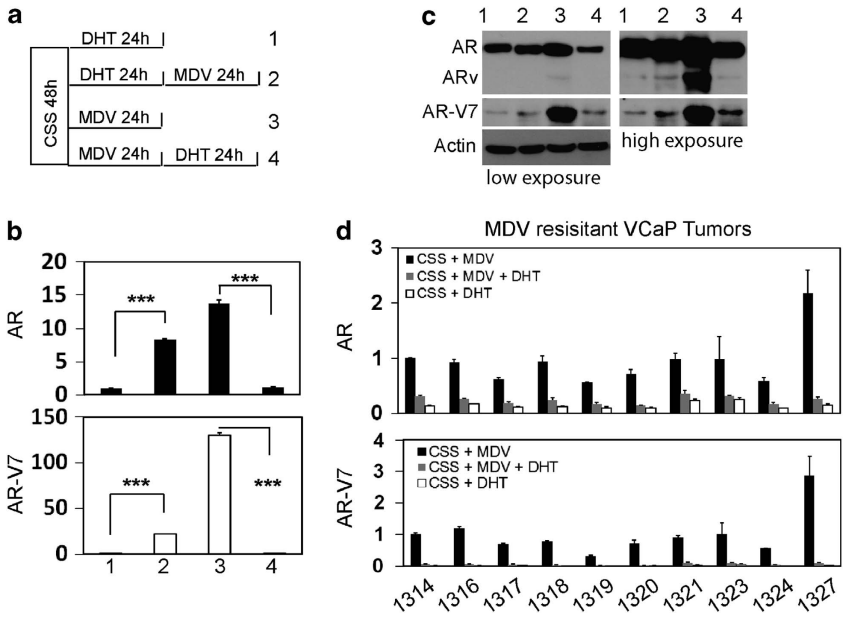

Figure 2. Alternative AR-V7 splicing is a reversible process regulated by AR signaling. (**a**) Schematic diagram of experimental design shows the treatments to VCaP cells. VCaP cells were maintained in RPMI1640 medium containing 5% CSS for 48 h. Cells were treated with 10 nM DHT (samples 1 and 2) or 5 μM MDV3100 (samples 3 and 4) for 24 h. Cells were washed and replenished with medium containing 5 μM MDV3100 (sample 2) or 10 nM DHT (sample 4) for another 24 h. RNA and protein samples were collected. (**b**) AR and AR-V7 mRNA level were measured by real-time qPCR using relative quantification to GAPDH. Results were obtained from three independent experiments with samples in triplicate and shown as mean ± s.e.m. Student's *t*-test showed statistical significances with $P<0.001$ as ***. (**c**) AR and AR-V7 protein levels were detected by western blotting assays. (**d**) Primary cultured MDV-resistant VCaP cells were described in Material and methods. Cells were treated with MDV3100, DHT or MDV3100 plus DHT for 24 h. Total RNA was collected and used to measure AR and AR-V7 RNA levels by real-time qPCR using relative quantitative method.

on AR when DHT was present. Consistent with cell proliferation assays, expression levels of prostate specific antigen (PSA) and transmembrane protease serine2 (TMPSS2) were further dramatically decreased by siRNAs targeting AR-V7 or total AR, when compared with siRNA targeting AR alone under androgen depletion and/or MDV treatment conditions (Figure 3b). In the presence of DHT, siRNA knocking down AR-V7 did not inhibit PSA and TMPSS2 expression. However, siRNA targeting total AR presented more potent suppressive effects to these genes when compared with siRNA targeting AR only. Interestingly, UGT2B17 and UBE2C were previously demonstrated to be AR-V7-regulated genes in PCa.[19] We further confirmed that AR-V7 was required for UGT2B17 transcription in VCaP cells under ADT conditions. In contrast, DHT-activated AR suppressed UGT2B17 RNA levels, which effects were blocked by AR knockdown. Similar observation was also from UBE2C expression that was inhibited by AR but enhanced by AR-V7 (Supplementary Figure 2). These findings indicate that under ADT conditions, AR-V7 can replace AR to sustain cell growth and regulate a gene set distinct from AR. Our results support a critical role of AR-V7 that is responsible for PCa phenotype shift from androgen sensitive to CRPC under castration stress. The efficiencies of siRNA knockdown of AR and or AR-V7 were shown by western blotting in Figure 3c. Together, our results indicate that AR-V7 maintains VCaP PCa cell proliferation by an AR signaling mechanism under ADT conditions.

AR-V7 RNA splicing is coupled with *AR* gene transcription

As the RNA splicing process was known to be coupled with gene transcription, and our data also indicated that AR-V7 RNA levels were correlated with AR RNA levels, we examined whether active AR-V7 splicing was controlled by the *AR* gene transcription rate. We applied three different approaches to inhibit *AR* gene transcription by treating cells with actinomycin D (ActD), benzimidazole (DRB) or trichostatin A (TSA). Cells were also co-treated with either 10 nM DHT or 5 μM MDV for 0, 1, 2, 4, 8 and 16 h (Figure 4). In the presence of vehicle, MDV maintained whereas DHT dramatically decreased both AR and AR-V7 RNA levels during 16 h of treatment in VCaP cells, while AR and AR-V7 RNA levels in LN95 cells were maintained at relatively constant levels. However, in both VCaP and LN95 cells, ActD and DRB eliminated, whereas TSA significantly reduced AR-V7 RNA levels correlating with changes of AR RNA levels. ActD forms complexes with double-stranded DNA to prevent RNA pol II from forming the transcription initiation complex, whereas DRB is an inhibitor of C-terminal domain of pol II that inhibits gene transcription at the elongation step. TSA was confirmed to inhibit *AR* gene transcription in several different PCa cell lines.[37,38] These results together indicated that AR-V7 splicing was dependent upon *AR* gene transcription initiation and elongation rates.

Recruitment, but not expression of RNA splicing factors, contributes to AR-V7 splicing

Although RNA splicing is coupled with transcription, generation of a RNA splice variant requires splicing factors that recognize and excise the alternative splice sites. We chose a panel of splicing factors including U1A, U2AF65, AFS/SF2, hnRNP I, PSF and p54nrb that were demonstrated to have essential roles in RNA splicing,[39] and measured their protein levels under DHT or MDV treatment. No changes in protein levels of these splicing factors were observed under different treatments and among different cell lines (Supplementary Figure 3).

We next determined whether recruitment of splicing factors to the *AR* gene was altered following ADT conditions. Chromatin immunoprecipitation (ChIP) assays were performed with primers amplifying the P1–P3 regions, corresponding to the 5′ and 3′ splice regions for AR and AR-V7 (Figure 5). The P4 region is located upstream of the 5′UTR (untranslated region) of human *GAPDH* gene, a region of the gene where there are no active RNA splicing

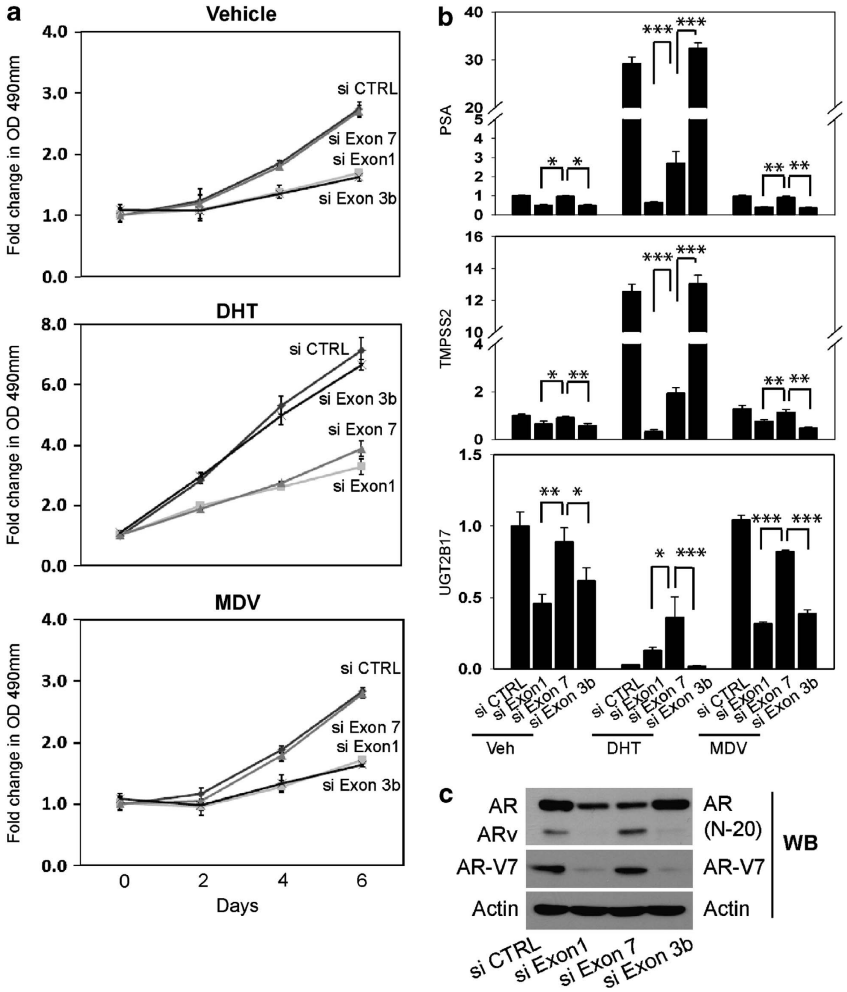

Figure 3. VCaP cells were transfected with control siRNA or siRNA targeting AR exon 1, exon 7 or exon 3B of the *AR* gene. (**a**) Cells were seeded in 96-well plates and treated with vehicle (Veh), 10 nM DHT or 5 μM MDV for 0–6 days. An MTS assay was performed at each time point. Data were plotted as fold change over day 0. (**b**) After siRNA transfections, VCaP cells were treated with Veh, DHT or MDV for another 24 h. Relative RNA levels of PSA, TMPSS2 and UGT2B17 over GAPDH were measured by real-time qPCR. (**c**) Efficiencies of siRNA knockdown were confirmed by western blotting assays with the indicated antibodies. $P<0.05$ as *, $P<0.01$ as ** and $P<0.001$ as ***.

events. It therefore serves as a negative control. Consistent with ADT-induced *AR* gene transcription, the recruitment of pol II to P1, P2 and P3 regions were significantly higher in MDV-treated VCaP cells. These changes were concurrent with increased recruitments of several RNA splicing factors (U1A, U2AF, ASF/SF2 and p54nrb) to P1, P2 and P3 regions. Exceptions were PSF (no change) and hnRNP I (decreased recruitment). These data suggested that MDV treatment increased spliceosome recruitment to the *AR* gene to process both AR and AR-V7 RNA splicing. In contrast, although MDV also enhanced pol II and U1A, U2AF and p54nrb onto P1 and P3 regions in LNCaP cells, their recruitments to the P2 region (containing AR-V7 3′ss) were not increased by MDV. These observations were consistent with low expression of AR-V7 in LNCaP cells. Together, these results suggested that spliceosome recruitment to the *AR* gene, rather than alterations in protein levels of splicing factors, contributed to AR-V7 splicing.

Construction of AR-V7 minigene to identify RNA splicing enhancers

In order to identify any *cis* and *trans* element responsible for AR-V7 splicing, we constructed the AR-V7 minigene plasmid (Figure 6a), with exon 3B and its flanking ~400-bp nucleotide sequence inserted in between exon 3 and exon 4 of the human *AR* gene. When transiently transfected, the minigene expressed 12–25 fold of AR and 8–300 fold of AR-V7 higher than the levels of endogenous AR transcripts in PCa cell lines (Figure 6b). Driven by the constitutively active CMV promoter, the levels of minigene transcribed AR-V7 were not affected by DHT or MDV treatment. These observations indicated that gene transcription rate, but not ADT condition *per se*, directly regulated AR-V7 RNA splicing.

To locate potential RNA sequences responsible for AR-V7 splicing, we screened exon 3B and its flanking region using the Splicing Rainbow[40] and ESEfinder 3.0[41] programs, two bioinformatic tools to predict potential splicing factor binding sites. One ISE and one ESE near the 3′ss of exon 3B were identified. The ISE was predicted to bind hnRNP I or U2AF65, whereas the ESE was a potential ASF/SF2 binding site. We applied mutagenesis and cloning techniques to further construct AR-V7 minigenes carrying point mutations at either ISE or ESE site (Figure 6c). When these mutant AR-V7 minigenes were introduced into PCa cells, only AR-V7 transcript levels, but not AR, were dramatically decreased (Figure 6d). To further confirm whether the functions of ISE and ESE were mediated through the predicted RNA splicing factors, we transfected AR-V7 minigenes into LNCaP cells in the presence of siRNAs against hnRNP I, U2AF65 and ASF/SF2. The levels of AR

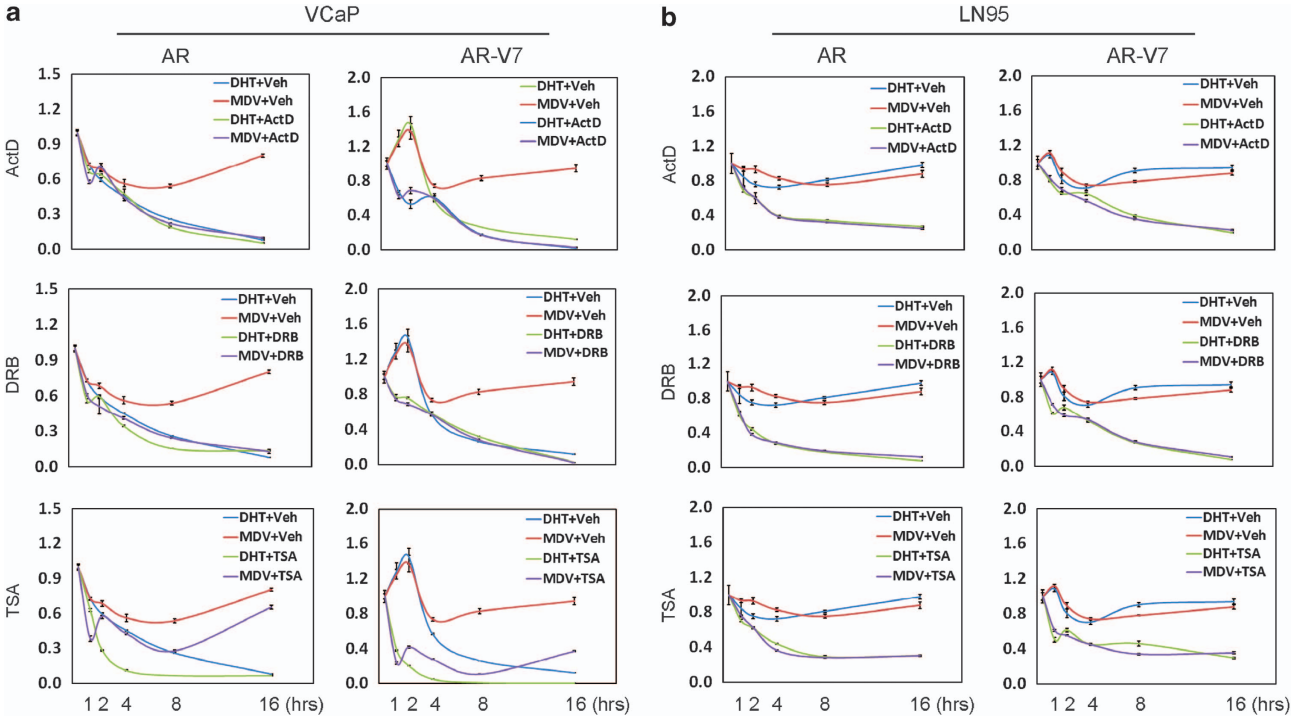

Figure 4. AR-V7 RNA splicing is coupled with *AR* gene transcription rate. VCaP (**a**) and LN95 (**b**) cells were maintained in RPMI1640 medium containing 5% CSS and treated with 10 nM DHT or 5 μM MDV3100 in the presence of vehicle (Veh), 1 μM ActD, 5 μM DRB or 10 nM TSA. RNA samples were collected at time points of 0, 1, 2, 4, 8 and 16 h. AR and AR-V7 RNA levels were determined by relative quantification to 18s rRNA. Results were obtained from two independent experiments with samples in triplicates and shown as mean ± s.e.m. Note: 18s rRNA levels were not altered by ActD, DRB or TSA treatment within 16 h, therefore, served as the internal control gene.

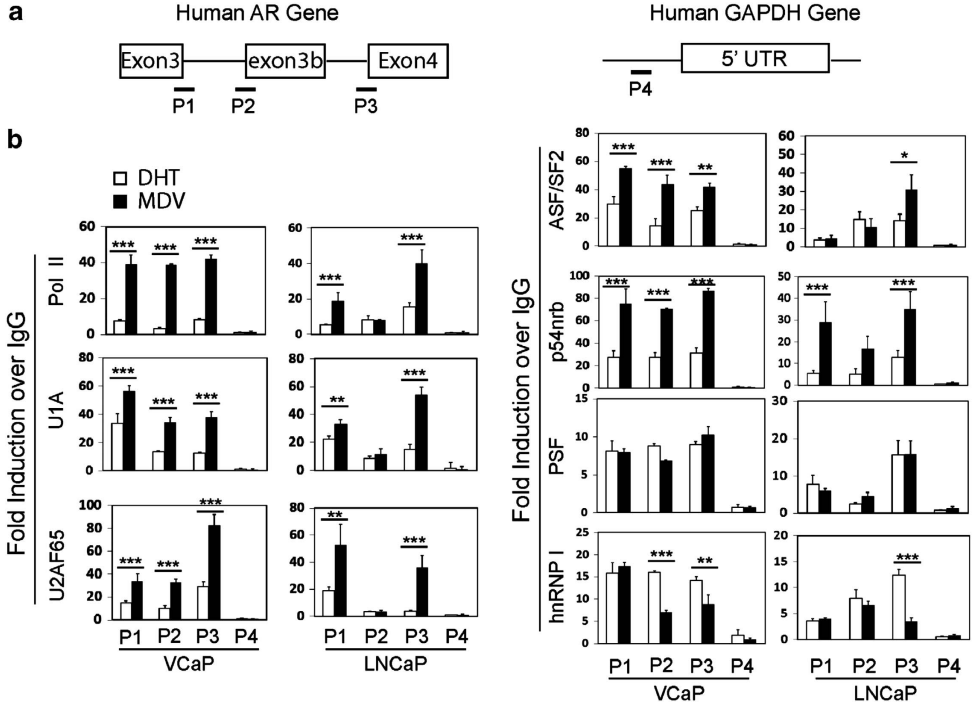

Figure 5. Recruitment of RNA splicing factors to the *AR* gene in PCa cells. (**a**) Schematic diagrams of the human *AR* gene and the *GAPDH* gene show the regions (P1–P4) that were amplified in ChIP assays. (**b**) VCaP and LNCaP cells were maintained in RPMI1640 medium containing 5% CSS for 48 h. Cells were treated with either 10 nM DHT or 5 μM MDV3100 for another 24 h. ChIP assays were performed using antibodies against pol II, U1A, U2AF65, ASF/SF2, p54nrb, PSF, hnRNP I and control IgG. Eluted DNA fragments were used as templates for real-time qPCR. Signals were calculated as percentage of input and blotted as fold changes over control IgG. ChIP data were derived from five independent experiments with triplicate samples per experiment. Student's *t*-test showed statistical significance with $P<0.05$ as *, $P<0.01$ as ** and $P<0.001$ as ***.

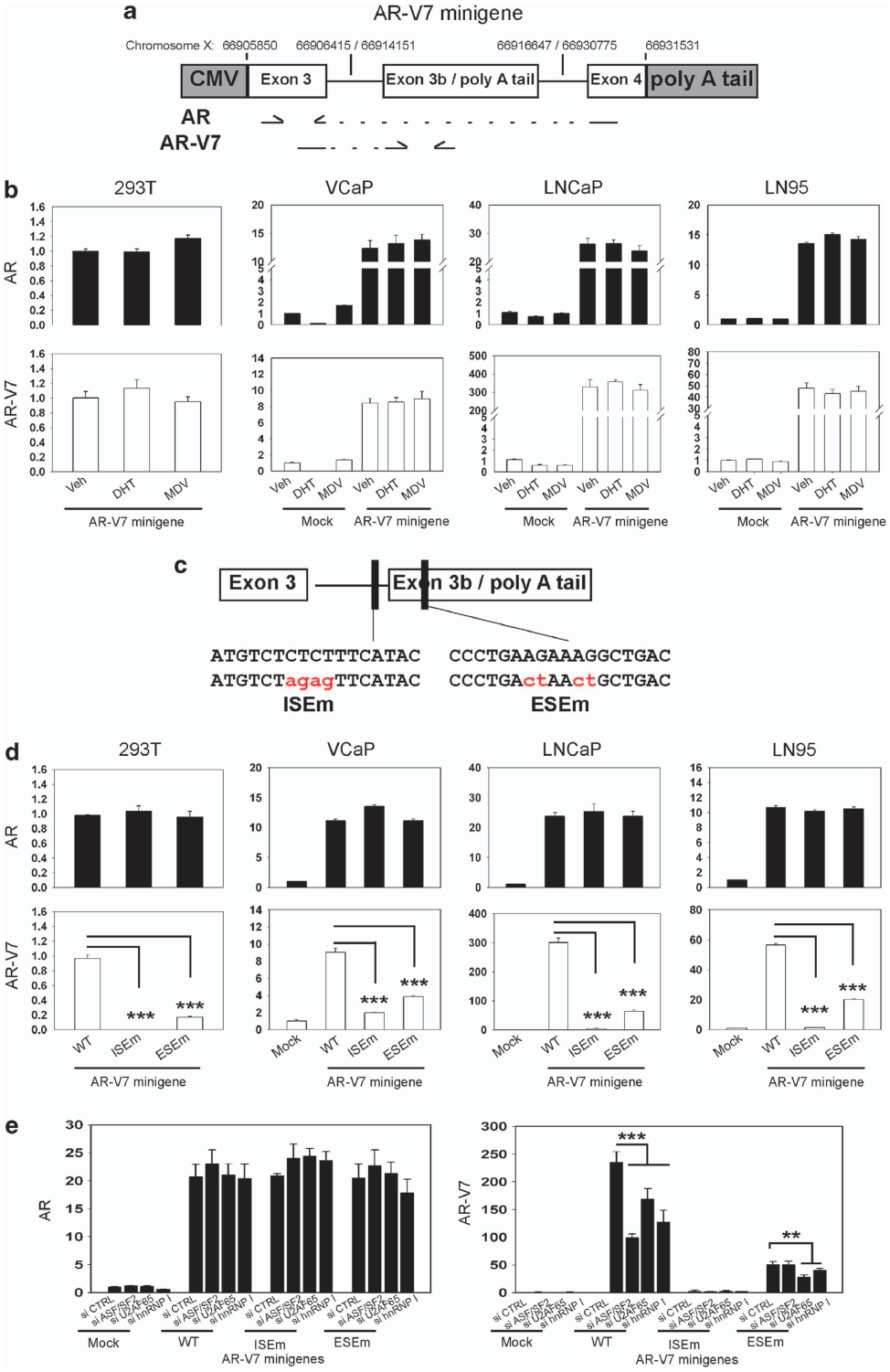

Figure 6. Construction of AR-V7 minigene to identify RNA splicing enhancers. (**a**) Schematic diagram of AR-V7 minigene construct and locations of primers used in real-time qPCR. Three DNA fragments of human *AR* gene were cloned into pCMV2 vectors. Positions of each *AR* gene fragment in the chromosome X were marked. (**b**) 293T, VCaP, LNCaP and LN95 cells were transiently transfected with mock vector or AR-V7 minigene plasmid. Cells were treated with vehicle (Veh), 10 nM DHT or 5 μM MDV3100 for 24 h. Relative mRNA levels of AR and AR-V7 mRNA levels to GAPDH were determined by real-time qPCR. (**c**) Using point mutagenesis, mutant AR-V7 mingenes were constructed with mutations at the ISE and the ESE sites. (**d**) 293T, VCaP, LNCaP and LN95 cells were transiently transfected with mock, AR-V7 minigene (WT) or AR-V7 minigenes with mutations at ISE (ISEm) and ESE (ESEm). (**e**) LNCaP cells were transfected with indicated siRNAs followed with plasmids encoding mock or AR minigenes (WT, ISEm or ESEm). Relative RNA levels of AR and AR-V7 to GAPDH were determined by real-time qPCR. Results were obtained from three independent experiments and shown as mean ± s.e.m. One-way ANOVA followed by Student's *t*-test was carried out using GraphPad Prism showing statistical significance with $P < 0.001$ as ***.

transcribed by AR-V7 minigenes were unchanged, regardless of siRNA knockdown or mutations at ESE or ISE within the minigenes (Figure 6e). In contrast, levels of AR-V7 transcribed by the AR-V7(WT) minigene were dramatically decreased with hnRNP I, U2AF65 or ASF/SF2 knockdown. The AR-V7(ISEm) minigene expressed very low levels of AR-V7, which were insensitive to any knockdown of splicing factors. Interestingly, RNA interference (RNAi) of U2AF65 and hnRNP I, but not ASF/SF2, further decreased AR-V7 levels transcribed by the AR-V7(ESEm) minigene. These findings indicated that both the ISE and the ESE were specifically important for AR-V7 splicing through interactions with U2AF65, hnRNP I and ASF/SF2.

Identification of RNA splicing factors responsible for AR-V7 splicing

To further study binding proteins for the ISE and the ESE, we synthesized two 40-bp RNA oligos to perform RNA pull-down assays (Figure 7a). Oligo 1 contains the ISE, whereas oligo 2 contains the ESE. Their sequences are listed in Supplementary Materials. Both oligos were incubated with purified Flag-tagged U2AF65, hnRNP I and ASF/SF2. hnRNP I and U2AF65 bound oligo 1. These interactions were abolished when the ISE was replaced with the ISEm (Figure 7b). Interestingly, hnRNP I and U2AF65 can also be pulled down by oligo 2. However, those interactions were not affected by ESE point mutations. ASF/SF2 had a strong association with oligo 2 but not with oligo 1. This interaction was also dramatically decreased when ESE was replaced with the ESEm. In order to show specific U2AF65/hnRNP I-ISE and ASF/SF2-ESE interactions, we also used oligos 1 and 2 to pull down two other RNA splicing factors, U1A and Tra2β. U1A bound both oligos 1 and 2 even in the presence of ISEm and ESEm, whereas Tra2β had no association to either RNA oligo. These results indicate that ASF/SF2 specifically binds the ESE, whereas hnRNP I and U2AF65 bind oligo 1 at the specific ISE site. They also bind oligo 2 but possibly through sequences other than the ESE.

RNA co-immunoprecipitation assays were further performed (Figure 7c). Antibodies against ASF/SF2, U2AF65 and hnRNP I, but not control immunoglobulin G (IgG), precipitated AR pre-mRNA at

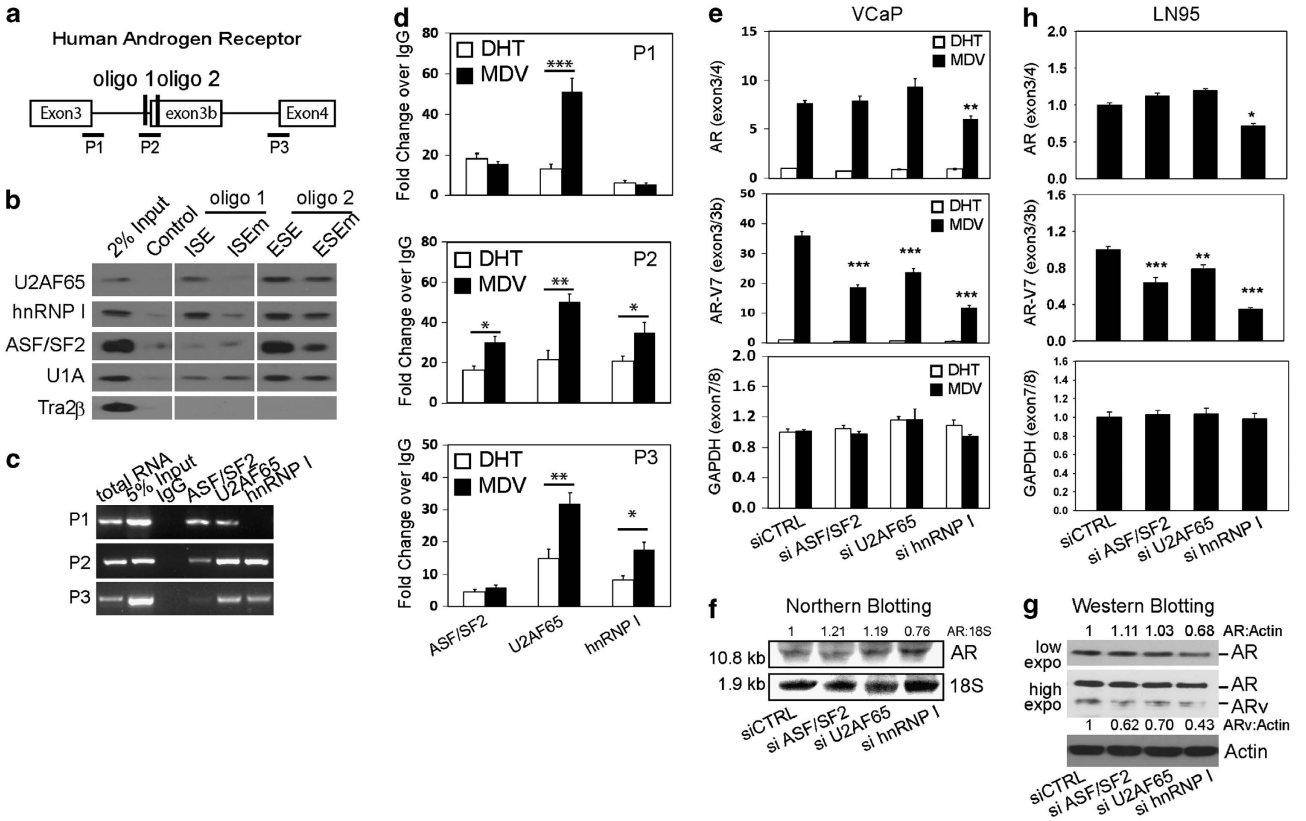

Figure 7. Characterization of RNA splicing factors that regulate AR-V7 splicing. (**a**) Schematic diagram of the *AR* gene between exon 3 and exon 4 and locations of AR pre-mRNA sequences used in RNA oligo pull-down assays (**b**) and primers used in RNA immunoprecipitation assays (**c** and **d**). (**b**) Flag-tagged purified RNA splicing factors U2AF65, hnRNP I, ASF/SF2, U1A and Tra2β were incubated with RNA oligos containing ISE, ESE and their point mutants. Oligo-associated splicing factors were detected by western blotting assays. (**c**) VCaP cell lysates were immunoprecipitated with antibodies against ASF/SF2, U2AF65 and hnRNP I. Protein associated pre-mRNA were extracted and reverse transcribed and analyzed by regular PCR with primers amplifying P1-3 regions. (**d**) VCaP cells were treated with either 10 nM DHT or 5 μM MDV3100 for 2 h. RNA immunoprecipitation assays were performed. Real-time qPCR quantified the enrichments of ASF/SF2, U2AF65 and hnRNP I on pre-mRNA at P1-3 regions. Signals were calculated as percentage of input and blotted as fold changes over control IgG. (**e**) VCaP cells were transfected with siRNAs against control, ASF/SF2, U2AF65 and hnRNP I for 48 h, after which cells were treated with either 10 nM DHT or 5 μM MDV3100 for another 24 h. AR and AR-V7 RNA splicing products were measured by real-time qPCR using relative quantification against GAPDH. A primer set covering GAPDH exon 7 and exon 8 was used as a negative control to monitor *GAPDH* gene splicing in response to RNAi of ASF/SF2, U2AF65 and hnRNP I. (**f** and **g**) AR protein and mRNA were also detected by western and northern blotting assays. Densitometry analyses calibrate RNA and protein bands of the *AR* gene by 18S and actin as the loading controls. In Figure 7g, both low and high exposures of western blot with AR(N-20) antibody were shown. (**h**) LN95 cells were transfected with siRNAs against controls ASF/SF2, U2AF65 and hnRNP I for 48 h. AR, AR-V7 and GAPDH splicing products were measured by real-time qPCR. Data were derived from three independent experiments and presented as mean ± s.e.m. One-way ANOVA followed by Student's *t*-test was carried out using GraphPad Prism showing statistical significance with $P<0.01$ as ** and $P<0.001$ as ***.

the P2 region (containing both the ISE and the ESE). Interestingly, hnRNP I was absent in the P1 region (5′ss for both AR and AR-V7) and ASF/SF2 showed an extremely low level at the P3 region (3′ss for AR). These observations suggest that hnRNP I functions primarily at the 3′ss, whereas ASF/SF2 has a relatively higher specificity to the 3′ss for AR-V7, emphasizing its important role for AR-V7 splicing. We further used real-time qPCR to quantify the recruitments of ASF/SF2, U2AF65 and hnRNP I to the AR pre-mRNA at the AR-V7 3′ss under DHT or MDV treatment for 2 h in VCaP cells (Figure 7d). MDV dramatically induced U2AF65 binding, but had no impact on ASF/SF2 and hnRNP I to the P1 region. However, all of these splicing factors had enhanced recruitment to the P2 region by MDV, whereas only U2AF65 and hnRNP I increased associations with the P3 region in response to MDV treatment. These results suggested that ASF/SF2-ESE and U2AF65/hnRNP I-ISE interactions were regulated by ADT condition in contributing to AR-V7 splicing.

To further confirm the functional significance of ASF/SF2, U2AF65 and hnRNP I for AR-V7 splicing, we knocked down each splicing factor in VCaP and LN95 cells, and measured AR and AR-V7 levels by real-time PCR amplifying exon 3/4 and exon 3/3B (Figures 7e and h). RNA silencing of ASF/SF2, U2AF65 and hnRNP I significantly reduced AR-V7 RNA levels. In addition, hnRNP I knockdown also mildly reduced AR levels. To exclude the possibility that ASF/SF2 and U2AF65 silencing also affect other splicing events particularly that within the *AR* gene, we further showed that U2AF65 and ASF/SF2 knockdown did not affect AR levels by both northern and western blotting (Figures 7f and g). In addition, we also designed a pair of primers crossing exons 7/8 of the *GAPDH* gene to measure its RNA splicing as a control, and showed that RNA splicing of the *GAPDH* gene was not affected by RNA silencing of ASF/SF2 and U2AF65. The efficiency of RNA silencing was shown by western blotting (Supplementary Figure 4). These results suggested that both ASF/SF2 and U2AF65, when compared with hnRNP I, were specifically important for AR-V7 splicing.

DISCUSSION

Although extensive studies show that constitutively transcriptional function of ARv is important for CRPC progression, the molecular mechanisms by which ARv is alternatively spliced remain unclear. Our studies demonstrate that *AR* gene transcription rates and splicing factor recruitment to AR pre-mRNA near the AR-V7 3′ss are two important factors contributing to AR-V7 splicing. The ADT condition does not directly regulate levels of AR-V7 splicing. Rather it enhances *AR* gene transcription rates and contributes indirectly to the generation of AR-V7 splice variant.

Our lines of evidence demonstrated that AR-V7 RNA synthesis depended upon active *AR* gene transcription. In various experimental conditions, changes in AR-V7 RNA levels were consistent with alterations of AR RNA levels in PCa cells. ADT induced the recruitment of RNA pol II to the *AR* gene, reflecting active *AR* gene transcription (Figure 4). Concurrently, higher AR and AR-V7 levels were observed under ADT conditions. Although ActD, DRB and TSA acted through different mechanisms to decrease *AR* gene transcription, they showed consistent repressive effects on AR-V7 RNA splicing (Figure 3). In addition, turning on or off of *AR* gene transcription by DHT and MDV reversibly controlled AR-V7 splicing (Figures 1 and 2). Previous publications showed that AR-V7 RNA was commonly expressed in PCa cells and even normal prostate epithelium cells,[13,15] and that the ratio of ARv:AR fluctuated between the 0.1–2.5% range depending upon active *AR* gene transcription by castration or DHT treatment.[36] These results together confirmed that AR-V7 RNA splicing process was coupled with *AR* gene transcription rate.

Although *AR* gene transcription provides a favorable genetic environment for AR-V7 RNA splicing, the enzymatic reaction to excise the 3′ss for AR-V7 splicing requires recruitment of RNA splicing factor to AR pre-mRNA for AR-V7 RNA synthesis. We showed that interactions of U2AF65-ISE and ASF/SF2-ESE were critical for this splicing event. Mutations at the ISE and the ESE abolished AR-V7 splicing, whereas RNA silencing of U2AF65 and ASF/SF2 decreased AR-V7 levels in both VCaP and LN95 cells. These results suggested that U2AF65 and ASF/SF2, by recognizing the ISE and the ESE, acted as the pioneer factors to direct further recruitment of RNA spliceosome to the AR-V7 3′ss. Although U2AF65 and ASF/SF2 might participate in other RNA splicing events, such as splicing the 3′ss next to exon 4 for AR, RNA silencing of U2AF65 and ASF/SF2 did not affect AR RNA levels nor did they affect the GAPDH (exon7/8) RNA splicing. Disruption of U2AF65-ISE or ASF/SF2-ESE interactions had no impact on AR RNA levels (Figure 5d). It is likely that the recruitment of U2AF65 and ASF/SF2 to the AR-V7 3′ss is more efficient because of the presence of the ESE and the ISE near the AR-V7 3′ss. ASF/SF2 is a concentration-dependent regulator for alternative RNA splicing. Although ADT does not alter its expression level, more AR pre-mRNA is available as a substrate for ASF/SF2 to catalyze RNA splicing reactions. The existence of ESE within the exon 3B therefore is more attractive for ASF/SF2 to be recruited to the AR-V7 3′ss and synthesize AR-V7 mRNA. In addition, the involvement of U2AF65 and ASF/SF2 in excising 3′ss next to exon 4 might be compensated by other splicing factors. As excision of the AR-V7 3′ss is more sensitive to U2AF65 and ASF/SF2 protein levels, they may serve as rate-limiting factors in controlling AR-V7 splicing efficiency. In contrast, although hnRNP I also binds the ISE, knocking down hnRNP I reduces both AR and AR-V7 levels, indicating hnRNP I serves as a general factor regulating both AR and AR-V7 splicing. Together, these results support that AR-V7 splicing is not generated by a random splicing error. Rather, it is executed by specific RNA splicing factors through recognizing specific RNA sequences near AR-V7 3′ss. This RNA splicing event is enhanced in response to ADT as AR transcription rates increase.

Our studies also demonstrated that neither *AR* gene amplification nor rearrangement were required for AR-V7 RNA splicing. Although VCaP cells have amplification of the *AR* gene, no such genetic aberrance is reported in LN95 cells. However, LN95 cells express comparable AR-V7 RNA levels. Regardless of *AR* gene amplification, suppression of the *AR* gene transcription rate or RNA silencing of splicing factors reduced AR-V7 splicing in both LN95 and VCaP cells. In VCaP, LNCaP and LN(AI) cells, AR-V7 RNA levels were repressed by DHT treatment (Figure 1). Particularly, AR-V7 RNA levels in VCaP cells can be reversibly regulated by DHT or MDV treatment within 24 h (Figure 2). These results indicate that *AR* gene amplification does not attribute to AR-V7 splicing. Rather, *AR* gene amplification magnifies the levels of all transcripts by the *AR* gene, supporting VCaP cells as an ideal model to study alternative RNA splicing events of the *AR* gene. Interestingly, both castration-resistant LN(AI) and LN95 cells express high levels of AR-V7 than their parent LNCaP cells, supporting the hypothesis that generation of AR-V7 contributes to CRPC progression.

An intragenic *AR* gene rearrangement was reported contributing to AR-V7 RNA synthesis in 22Rv1 cells.[42] No such gene rearrangement was noted in VCaP or castration-resistant LN(AI) and LN95 cells.[35] It could be possible that similar genomic disruption may exist in some other PCa cells. However, AR-V7 mRNA synthesis still requires the removal of intron sequences through the RNA splicing process. RNA splicing factors still need to recognize and excise the 3′ss, and ligate the exon 3 with exon 3B. This enzymatic reaction will depend on active *AR* gene transcription to create a permissible environment and recruitment of splicing factors to AR pre-mRNA. Our data showed that changes in recruitment of U2AF65 and ASF/SF2 occurred within 2 h of MDV treatment (Figure 6d). Enhanced AR-V7 RNA levels by MDV can be lowered within hours by subsequent DHT treatment (Figures 2a and b), indicating that AR-V7 RNA splicing is a dynamic and reversible process.

In summary, our data provide new insights to the complexity of *AR* gene splicing during CRPC progression of PCa. It invites further investigation that may lead to therapeutic revenues to block AR-V7 expression in CRPC tumors and resensitize current anti-AR therapy.

MATERIALS AND METHODS

Cell culture

The human PCa cell line VCaP (CRL-2876) was purchased from ATCC (Manassas, VA, USA) and LNCaP, C4-2B, LN(AI) and 293T cell lines were generously provided by Drs Gleave, Rennie and Buttyan from the Vancouver Prostate Centre. LN95 cells were described previously and were a generous gift from Dr Alan Meeker of Johns Hopkins University.[18] VCaP and 293T cells were cultured in DMEM, whereas LNCaP and C4-2B cells were cultured in RPMI1640 medium. LN(AI) and LN95 cells were maintained in RPMI1640 medium with charcoal-stripped serum (CSS). CSS was used for steroid studies (Hyclone, Logan, UT, USA). DHT, ActD, DRB and TSA were purchased from Cedarlane (Burlington, ON, Canada). MDV3100 was from Haoyuan Chemexpress (Shanghai, China). Plasmids encoding Flag-tagged RNA splicing factor are U2AF65 (Dr James Manley, Columbia University), ASF/SF2 (Dr Gourisankar Ghosh, UC San Diego), hnRNP I (Dr Allain Frédéric, Institute for Molecular Biology and Biophysics Eidgenössiche Technische Hochshule, Switzerland) and Tra2β (Dr Stefan Stamm, University of Kentucky).

Reverse-transcriptase PCR and real-time qPCR

Total RNA was extracted using TRIZOL reagent (Invitrogen, Burlington, ON, Canada) and treated with deoxyribonuclease at room temperature for 15 min to eliminate any DNA contamination. The reverse transcription reaction was performed using random hexamers and superscript II (Invitrogen), after which the product was used as a template for PCR. Real-time qPCR was performed on the ABI PRISM 7900 HT system (Applied Biosystems, Burlington, ON, Canada) using the FastStart Universal SYBR Green Master mix (Roche, Laval, QU, Canada) as we previously reported.[43] Cycling was performed using default conditions of the 7900HT Software (Applied Biosystems)—2 min at 50 °C and 10 min at 95 °C—followed by 40 cycles of 15 s at 95 °C and 1 min at 60 °C. Absolute quantification followed the previous report,[44] AR and AR-V7 cDNAs were quantified by NanoDrop (Thermo Scientific, Wilmington, DE, USA), and their copy numbers were calculated by copy number (molecules/μl) = concentration(g/μl)/(bp size of double-stranded product $\times 660) \times 6.022 \times 10^{23}$. A series of dilutions of the cDNAs were used as templates for real-time qPCR as standards for AR or AR-V7. A standard curve was drawn by plotting the C_T value against the log of the copy number of molecules. The specific AR and AR-V7 copy numbers were calculated by the equation drawn from the graph. The relative quantification method has been described before using GAPDH or 18s rRNA as the internal control genes.[43] All real-time qPCR assays were carried out using three technical replications, as well as three independent cDNA syntheses. Primer information is listed in the Supplementary Materials.

Western blot and ChIP

After treatments, cells were incubated with lysis buffer (50 mM Tris pH8.0, 150 mM NaCl, 1% NP40, 0.5% sodium deoxycholate and 0.1% SDS) followed by a brief sonication to extract protein lysate. Lysates were immunoblotted with specific antibodies (detailed in Supplementary Materials). ChIP assays followed the protocol that we previously reported.[43,45] DNA templates retrieved from ChIP were analyzed by real-time qPCR on the ABI PRISM 7900 HT system (Applied Biosystems) using the FastStart Universal SYBR Green Master (Roche). Enrichments of immunoprecipitated DNA fragments were determined by the threshold cycle (Ct) value. Data were calculated as a percentage of input and plotted as fold changes over control IgG. ChIP data were derived from five independent experiments with samples in triplicate. Data are presented as mean ± s.e.m.

MDV-resistant VCaP xenografts

MDV-resistant xenografts of VCaP cells were generated by injecting VCaP cells subcutaneously in castrate SCID (severe combined immunodeficiency) mice (2×10^6 cells mixed 1:1 with Matrigel). When xenograft tumors reached 500–800 mm^3, the animals were euthanized, tumors were removed, collagenase were digested and again injected subcutaneously into castrate SCID mice 1:1 with Matrigel. Mice were treated with MDV3100 (10 mgm/kg) per gavage 5 days a week. When xenografts reached 800–1000 mm^3, mice were euthanized, tumors were final minced and 1/3 of each minced tumor was grown in a 100-mm plastic culture dish with RPMI1640 plus 5% CSS and 5 μM gentamicin. Cells were treated with 10 μM MDV3100, 1 nM DHT or MDV3100 plus DHT for 24 h. Total RNA was collected to measure AR and AR-V7 RNA levels by real-time qPCR. All animal studies were approved by the University of Washington Institutional Animal Care and Use Committee (IACUC).

Transfection and RNA silencing

Transient transfection of plasmid DNA used the Lipofectamine 2000 (Invitrogen). Transfection of siRNA oligos used the siLentFect Lipid Reagent (Bio-Rad, Mississauga, ON, Canada) according to the provided protocols.

Cell proliferation assay

VCaP PCa cells were first transfected with siRNA against the *AR* gene at indicated exons. Cells were seeded in 96-well plates (5000 cells/well) with culture medium containing 10% CSS for another 24 h. Cells were then treated with vehicle, DHT or MDV3100, for 0–6 days. The reagent of 3-(4, 5-dimethylthiazol-2-yl)-5-(3-carboxymethoxyphenyl)-2-(4-sulfophenyl)-2Htetrazolium (Promega, Madison, WI, USA) was added at each time point. Cell proliferation rates were measured according to the manufacturer's protocol.

AR-V7 minigene construction

The human genomic BAC clone (RP11-75E16) was provided by The Centre for Applied Genomics, The Hospital for Sick Children, University of Toronto. It was used as the template for PCR to amplify exon 3, exon 3B and exon 4, and their flanking intron regions (~300–400 base pairs) by Platinum Taq DNA Polymerase High Fidelity (Invitrogen). Three DNA fragments were cloned into the plasmid vector pCMV2 (Sigma, Oakville, Ontario, Canada) between the *Eco*RI and *Sal*I sites. Full sequences of the vectors will be provided upon request. DNA sequencing confirmed the integrity of the final AR-V7 construct. DNA mutagenesis was further performed using the AR-V7 minigene as the template to construct AR-V7 (ESEm) and AR-V7 (ISEm).

RNA protein interaction assay

RNA oligo pull down was performed by first immobilizing 0.4 nmol biotin-labeled RNA oligonucleotides (Invitrogen) onto 100 μl of streptavidin beads (Pierce, Rockford, IL, USA) in a final volume of 500 μl of binding buffer (20 mM HEPES-KOH, pH 7.9, 80 mM potassium glutamate, 0.1 mM EDTA, 1 mM DTT and 20% glycerol) at 4 °C for 2 h. RNA splicing factors, U2AF65, ASF/SF2, hnRNP I, U1A and Tra2β proteins, were purified by transfecting plasmids encoding Flag-tagged splicing factors into 293T cells, followed with purification using Anti-Flag M2 Affinity gel (Sigma) as reported.[45] The immobilized RNA oligos were then incubated with 50 μg-purified splicing factors in binding buffer containing 30 U/ml RNase OUT and 15 μg/ml yeast tRNA in a final volume of 400 μl at 4 °C for 2 h. The beads were washed three times with binding buffer and once with washing buffer (20 mM HEPES-KOH, pH 7.9, 0.1 mM EDTA, 1 mM DTT, 75 mM KCl and 20% glycerol), and suspended in 40 μl of 2 × sodium dodecyl sulfate sample buffer and boiled for 5 min. Eluted proteins were analyzed by western blot. RNA oligo sequences are listed in Supplementary Materials.

RNA co-immunoprecipitation

RNA co-immunoprecipitations were performed as previously reported[46,47] with the following modifications. Cell nuclei were first extracted by isotonic buffer (10 mM Tris/HCl, pH 7.4, 10 mM NaCl, 2.5 mM $MgCl_2$, 1 mM DTT, protease inhibitor cocktail, 30 U/ml RNase OUT, 10 mM β-glycerophosphate and 0.5 mM $NaVO_4$). After incubation on ice for 7 min, nuclei were collected by centrifugation at 700 *g* for 7 min, re-suspended in isotonic buffer supplemented with 90 mM of NaCl and 0.5% Triton X-100, and briefly sonicated. Soluble nuclear extracts were first precleared with protein A/G-Sepharose beads (Santa Cruz, Dallas, TX, USA) and control IgGs, then immunoprecipitated with 2 μg of ASF/SF2, hnRNP I or U2AF65 antibody. After extensive washes by isotonic buffer, the precipitated antibody–antigen complexes were first incubated with DNase I (RNase free, Ambion, Burlington, ON, Canada) for 15 min at 37 °C, followed with 50 μg of proteinase K (Roche) treatment for 15 min at 37 °C. Co-precipitated RNA was then extracted by TRIzol and used for cDNA synthesis and PCR

analyses. Enrichment of precipitated RNA was determined by the Ct value. Data were calculated as percentage of input and plotted as fold changes over control IgG. RNA co-immunoprecipitation data were derived from three independent experiments with samples in triplicate. Results were presented as mean ± s.e.m.

Northern blotting

VCaP cells were transfected with control siRNA or siRNA against U2AF65, ASF/SF2 and hnRNP I for 48 h. Total RNA was extracted by using Trizol (Invitrogen). Twenty microgram of total RNA were used for northern blotting analysis to detect AR and 18S RNA levels as described.[48]

Statistics

Data were presented as mean ± s.e.m. that were calculated from three or more different experiments. Statistical significances were calculated by using one-way analysis of variance (ANOVA) and paired Student's *t*-test. A *P*-value of <0.05 was considered significant. *represents $P<0.05$, **represents $P<0.01$ and ***represents $P<0.001$.

CONFLICT OF INTEREST

The authors declare no conflict of interest.

ACKNOWLEDGEMENTS

This study was supported by Pacific Northwest Prostate Cancer SPORE, National Cancer Institute (P50CA097186; XD and SRP); Prostate Cancer Canada (RS2013-58; to XD) and Canadian Institute of Health Research (MOP-97934; XD); Department of Defence plus Veterans Administration Grants (SRP), NIH P01 CA163227 (SRP) and Prostate Cancer Foundation (SRP).

REFERENCES

1 Sims 3rd RJ, Millhouse S, Chen CF, Lewis BA, Erdjument-Bromage H, Tempst P *et al.* Recognition of trimethylated histone H3 lysine 4 facilitates the recruitment of transcription postinitiation factors and pre-mRNA splicing. *Mol Cell* 2007; **28**: 665–676.
2 Chen Y, Clegg NJ, Scher HI. Anti-androgens and androgen-depleting therapies in prostate cancer: new agents for an established target. *Lancet Oncol* 2009; **10**: 981–991.
3 Scher HI, Sawyers CL. Biology of progressive, castration-resistant prostate cancer: directed therapies targeting the androgen-receptor signaling axis. *J Clin Oncol* 2005; **23**: 8253–8261.
4 Chen CD, Welsbie DS, Tran C, Baek SH, Chen R, Vessella R *et al.* Molecular determinants of resistance to antiandrogen therapy. *Nat Med* 2004; **10**: 33–39.
5 Taplin ME, Balk SP. Androgen receptor: a key molecule in the progression of prostate cancer to hormone independence. *J Cell Biochem* 2004; **91**: 483–490.
6 Locke JA, Guns ES, Lubik AA, Adomat HH, Hendy SC, Wood CA *et al.* Androgen levels increase by intratumoral de novo steroidogenesis during progression of castration-resistant prostate cancer. *Cancer Res* 2008; **68**: 6407–6415.
7 Mostaghel EA, Page ST, Lin DW, Fazli L, Coleman IM, True LD *et al.* Intraprostatic androgens and androgen-regulated gene expression persist after testosterone suppression: therapeutic implications for castration-resistant prostate cancer. *Cancer Res* 2007; **67**: 5033–5041.
8 Heemers HV, Schmidt LJ, Kidd E, Raclaw KA, Regan KM, Tindall DJ. Differential regulation of steroid nuclear receptor coregulator expression between normal and neoplastic prostate epithelial cells. *Prostate* 2010; **70**: 959–970.
9 Sadar MD. Androgen-independent induction of prostate-specific antigen gene expression via cross-talk between the androgen receptor and protein kinase A signal transduction pathways. *J Biol Chem* 1999; **274**: 7777–7783.
10 Dehm SM, Schmidt LJ, Heemers HV, Vessella RL, Tindall DJ. Splicing of a novel androgen receptor exon generates a constitutively active androgen receptor that mediates prostate cancer therapy resistance. *Cancer Res* 2008; **68**: 5469–5477.
11 Hu R, Dunn TA, Wei S, Isharwal S, Veltri RW, Humphreys E *et al.* Ligand-independent androgen receptor variants derived from splicing of cryptic exons signify hormone-refractory prostate cancer. *Cancer Res* 2009; **69**: 16–22.
12 Hu R, Isaacs WB, Luo J. A snapshot of the expression signature of androgen receptor splicing variants and their distinctive transcriptional activities. *Prostate* 2011; **71**: 1656–1667.
13 Guo Z, Yang X, Sun F, Jiang R, Linn DE, Chen H *et al.* A novel androgen receptor splice variant is up-regulated during prostate cancer progression and promotes androgen depletion-resistant growth. *Cancer Res* 2009; **69**: 2305–2313.
14 Yang X, Guo Z, Sun F, Li W, Alfano A, Shimelis H *et al.* Novel membrane-associated androgen receptor splice variant potentiates proliferative and survival responses in prostate cancer cells. *J Biol Chem* 2011; **286**: 36152–36160.
15 Sun S, Sprenger CC, Vessella RL, Haugk K, Soriano K, Mostaghel EA *et al.* Castration resistance in human prostate cancer is conferred by a frequently occurring androgen receptor splice variant. *J Clin Invest* 2010; **120**: 2715–2730.
16 Li Y, Chan SC, Brand LJ, Hwang TH, Silverstein KA, Dehm SM. Androgen receptor splice variants mediate enzalutamide resistance in castration-resistant prostate cancer cell lines. *Cancer Res* 2013; **73**: 483–489.
17 Cai C, He HH, Chen S, Coleman I, Wang H, Fang Z *et al.* Androgen receptor gene expression in prostate cancer is directly suppressed by the androgen receptor through recruitment of lysine-specific demethylase 1. *Cancer Cell* 2011; **20**: 457–471.
18 Hu R, Lu C, Mostaghel EA, Yegnasubramanian S, Gurel M, Tannahill C *et al.* Distinct transcriptional programs mediated by the ligand-dependent full-length androgen receptor and its splice variants in castration-resistant prostate cancer. *Cancer Res* 2012; **72**: 3457–3462.
19 Zhang X, Morrissey C, Sun S, Ketchandji M, Nelson PS, True LD *et al.* Androgen receptor variants occur frequently in castration resistant prostate cancer metastases. *PLoS ONE* 2011; **6**: e27970.
20 Hornberg E, Ylitalo EB, Crnalic S, Antti H, Stattin P, Widmark A *et al.* Expression of androgen receptor splice variants in prostate cancer bone metastases is associated with castration-resistance and short survival. *PLoS ONE* 2011; **6**: e19059.
21 Srebrow A, Kornblihtt AR. The connection between splicing and cancer. *J Cell Sci* 2006; **119**(Pt 13): 2635–2641.
22 Goldstrohm AC, Greenleaf AL, Garcia-Blanco MA. Co-transcriptional splicing of pre-messenger RNAs: considerations for the mechanism of alternative splicing. *Gene* 2001; **277**: 31–47.
23 Chew SL, Liu HX, Mayeda A, Krainer AR. Evidence for the function of an exonic splicing enhancer after the first catalytic step of pre-mRNA splicing. *Proc Natl Acad Sci USA.* 1999; **96**: 10655–10660.
24 Chen M, Manley JL. Mechanisms of alternative splicing regulation: insights from molecular and genomics approaches. *Nat Rev Mol Cell Biol* 2009; **10**: 741–754.
25 Kornblihtt AR. Coupling transcription and alternative splicing. *Adv Exp Med Biol* 2007; **623**: 175–189.
26 Auboeuf D, Honig A, Berget SM, O'Malley BW. Coordinate regulation of transcription and splicing by steroid receptor coregulators. *Science* 2002; **298**: 416–419.
27 Nogues G, Kadener S, Cramer P, Bentley D, Kornblihtt AR. Transcriptional activators differ in their abilities to control alternative splicing. *J Biol Chem* 2002; **277**: 43110–43114.
28 Batsche E, Yaniv M, Muchardt C. The human SWI/SNF subunit Brm is a regulator of alternative splicing. *Nat Struct Mol Biol* 2006; **13**: 22–29.
29 McCracken S, Fong N, Yankulov K, Ballantyne S, Pan G, Greenblatt J *et al.* The C-terminal domain of RNA polymerase II couples mRNA processing to transcription. *Nature* 1997; **385**: 357–361.
30 Maniatis T, Reed R. An extensive network of coupling among gene expression machines. *Nature* 2002; **416**: 499–506.
31 Moore MJ, Proudfoot NJ. Pre-mRNA processing reaches back to transcription and ahead to translation. *Cell* 2009; **136**: 688–700.
32 Luco RF, Allo M, Schor IE, Kornblihtt AR, Misteli T. Epigenetics in alternative pre-mRNA splicing. *Cell* 2011; **144**: 16–26.
33 Kornblihtt AR. Promoter usage and alternative splicing. *Curr Opin Cell Biol* 2005; **17**: 262–268.
34 Kadener S, Cramer P, Nogues G, Cazalla D, de la Mata M, Fededa JP *et al.* Antagonistic effects of T-Ag and VP16 reveal a role for RNA pol II elongation on alternative splicing. *EMBO J.* 2001; **20**: 5759–5768.
35 Li Y, Hwang TH, Oseth LA, Hauge A, Vessella RL, Schmechel SC *et al.* AR intragenic deletions linked to androgen receptor splice variant expression and activity in models of prostate cancer progression. *Oncogene* 2012; **31**: 4759–4767.
36 Watson PA, Chen YF, Balbas MD, Wongvipat J, Socci ND, Viale A *et al.* Constitutively active androgen receptor splice variants expressed in castration-resistant prostate cancer require full-length androgen receptor. *Proc Natl Acad Sci USA.* 2010; **107**: 16759–16765.
37 Welsbie DS, Xu J, Chen Y, Borsu L, Scher HI, Rosen N *et al.* Histone deacetylases are required for androgen receptor function in hormone-sensitive and castrate-resistant prostate cancer. *Cancer Res* 2009; **69**: 958–966.
38 Rokhlin OW, Glover RB, Guseva NV, Taghiyev AF, Kohlgraf KG, Cohen MB. Mechanisms of cell death induced by histone deacetylase inhibitors in androgen receptor-positive prostate cancer cells. *Mol Cancer Res* 2006; **4**: 113–123.

39 Caceres JF, Kornblihtt AR. Alternative splicing: multiple control mechanisms and involvement in human disease. *Trends Genet* 2002; **18**: 186–193.
40 Stamm S, Riethoven JJ, Le Texier V, Gopalakrishnan C, Kumanduri V, Tang Y *et al.* ASD: a bioinformatics resource on alternative splicing. *Nucleic Acids Rese* 2006; **34**(Database issue): D46–D55.
41 Cartegni L, Wang J, Zhu Z, Zhang MQ, Krainer AR. ESEfinder: A web resource to identify exonic splicing enhancers. *Nucleic Acids Res* 2003; **31**: 3568–3571.
42 Li Y, Alsagabi M, Fan D, Bova GS, Tewfik AH, Dehm SM. Intragenic rearrangement and altered RNA splicing of the androgen receptor in a cell-based model of prostate cancer progression. *Cancer Res* 2011; **71**: 2108–2117.
43 Xie N, Liu L, Li Y, Yu C, Lam S, Shynlova O *et al.* Expression and function of myometrial PSF suggest a role in progesterone withdrawal and the initiation of labor. *Mol Endocrinol* 2012; **26**: 1370–1379.
44 Luco RF, Pan Q, Tominaga K, Blencowe BJ, Pereira-Smith OM, Misteli T. Regulation of alternative splicing by histone modifications. *Science* 2010; **327**: 996–1000.
45 Dong X, Sweet J, Challis JR, Brown T, Lye SJ. Transcriptional activity of androgen receptor is modulated by two RNA splicing factors, PSF and p54nrb. *Mol Cell Biol* 2007; **27**: 4863–4875.
46 Olshavsky NA, Comstock CE, Schiewer MJ, Augello MA, Hyslop T, Sette C *et al.* Identification of ASF/SF2 as a critical, allele-specific effector of the cyclin D1b oncogene. *Cancer Res* 2010; **70**: 3975–3984.
47 Paronetto MP, Achsel T, Massiello A, Chalfant CE, Sette C. The RNA-binding protein Sam68 modulates the alternative splicing of Bcl-x. *J Cell Biol* 2007; **176**: 929–939.
48 Cheng H, Snoek R, Ghaidi F, Cox ME, Rennie PS.. Short hairpin RNA knockdown of the androgen receptor attenuates ligand-independent activation and delays tumor progression. *Cancer Res* 2006; **66**: 10613–10620.

Supplementary Information accompanies this paper on the Oncogene website (http://www.nature.com/onc)